Indian Ocean Biogeochemical Processes and Ecological Variability

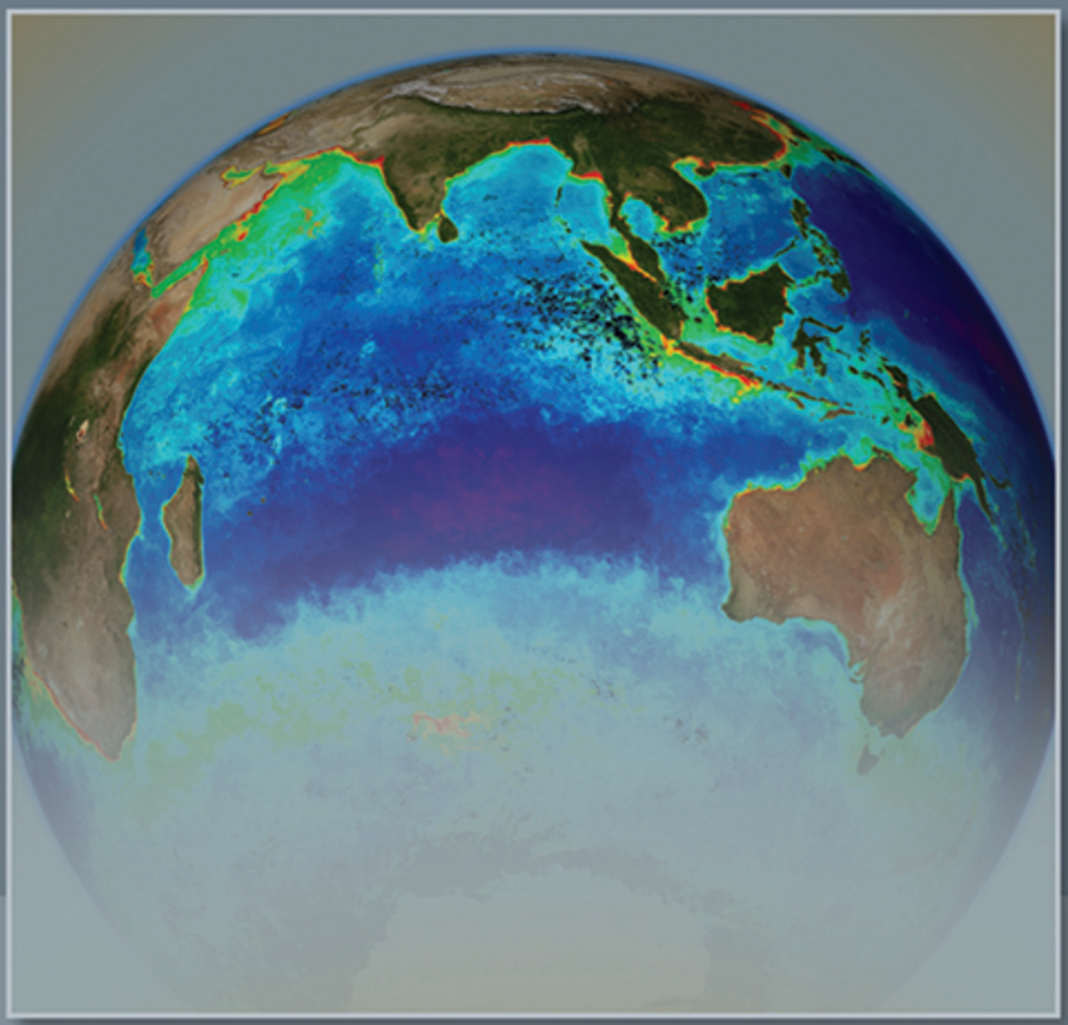

Jerry D. Wiggert, Raleigh R. Hood, S. Wajih A. Naqvi,
Kenneth H. Brink, and Sharon L. Smith
Editors

AGU

Geophysical Monograph Series

Including
IUGG Volumes
Maurice Ewing Volumes
Mineral Physics Volumes

150 **The State of the Planet: Frontiers and Challenges in Geophysics** *Robert Stephen John Sparks, and Christopher John Hawkesworth (Eds.)*

151 **The Cenozoic Southern Ocean: Tectonics, Sedimentation, and Climate Change Between Australia and Antarctica** *Neville Exon, James P. Kennett and Mitchell Malone (Eds.)*

152 **Sea Salt Aerosol Production: Mechanisms, Methods, Measurements, and Models** *Ernie R. Lewis and Stephen E. Schwartz*

153 **Ecosystems and Land Use Change** *Ruth S. DeFries, Gregory P. Anser, and Richard A. Houghton (Eds.)*

154 **The Rocky Mountain Region—An Evolving Lithosphere: Tectonics, Geochemistry, and Geophysics** *Karl E. Karlstrom and G. Randy Keller (Eds.)*

155 **The Inner Magnetosphere: Physics and Modeling** *Tuija I. Pulkkinen, Nikolai A. Tsyganenko, and Reiner H. W. Friedel (Eds.)*

156 **Particle Acceleration in Astrophysical Plasmas: Geospace and Beyond** *Dennis Gallagher, James Horwitz, Joseph Perez, Robert Preece, and John Quenby (Eds.)*

157 **Seismic Earth: Array Analysis of Broadband Seismograms** *Alan Levander and Guust Nolet (Eds.)*

158 **The Nordic Seas: An Integrated Perspective** *Helge Drange, Trond Dokken, Tore Furevik, Rüdiger Gerdes, and Wolfgang Berger (Eds.)*

159 **Inner Magnetosphere Interactions: New Perspectives From Imaging** *James Burch, Michael Schulz, and Harlan Spence (Eds.)*

160 **Earth's Deep Mantle: Structure, Composition, and Evolution** *Robert D. van der Hilst, Jay D. Bass, Jan Matas, and Jeannot Trampert (Eds.)*

161 **Circulation in the Gulf of Mexico: Observations and Models** *Wilton Sturges and Alexis Lugo-Fernandez (Eds.)*

162 **Dynamics of Fluids and Transport Through Fractured Rock** *Boris Faybishenko, Paul A. Witherspoon, and John Gale (Eds.)*

163 **Remote Sensing of Northern Hydrology: Measuring Environmental Change** *Claude R. Duguay and Alain Pietroniro (Eds.)*

164 **Archean Geodynamics and Environments** *Keith Benn, Jean-Claude Mareschal, and Kent C. Condie (Eds.)*

165 **Solar Eruptions and Energetic Particles** *Natchimuthukonar Gopalswamy, Richard Mewaldt, and Jarmo Torsti (Eds.)*

166 **Back-Arc Spreading Systems: Geological, Biological, Chemical, and Physical Interactions** *David M. Christie, Charles Fisher, Sang-Mook Lee, and Sharon Givens (Eds.)*

167 **Recurrent Magnetic Storms: Corotating Solar Wind Streams** *Bruce Tsurutani, Robert McPherron, Walter Gonzalez, Gang Lu, José H. A. Sobral, and Natchimuthukonar Gopalswamy (Eds.)*

168 **Earth's Deep Water Cycle** *Steven D. Jacobsen and Suzan van der Lee (Eds.)*

169 **Magnetospheric ULF Waves: Synthesis and New Directions** *Kazue Takahashi, Peter J. Chi, Richard E. Denton, and Robert L. Lysal (Eds.)*

170 **Earthquakes: Radiated Energy and the Physics of Faulting** *Rachel Abercrombie, Art McGarr, Hiroo Kanamori, and Giulio Di Toro (Eds.)*

171 **Subsurface Hydrology: Data Integration for Properties and Processes** *David W. Hyndman, Frederick D. Day-Lewis, and Kamini Singha (Eds.)*

172 **Volcanism and Subduction: The Kamchatka Region** *John Eichelberger, Evgenii Gordeev, Minoru Kasahara, Pavel Izbekov, and Johnathan Lees (Eds.)*

173 **Ocean Circulation: Mechanisms and Impacts—Past and Future Changes of Meridional Overturning** *Andreas Schmittner, John C. H. Chiang, and Sidney R. Hemming (Eds.)*

174 **Post-Perovskite: The Last Mantle Phase Transition** *Kei Hirose, John Brodholt, Thorne Lay, and David Yuen (Eds.)*

175 **A Continental Plate Boundary: Tectonics at South Island, New Zealand** *David Okaya, Tim Stem, and Fred Davey (Eds.)*

176 **Exploring Venus as a Terrestrial Planet** *Larry W. Esposito, Ellen R. Stofan, and Thomas E. Cravens (Eds.)*

177 **Ocean Modeling in an Eddying Regime** *Matthew Hecht and Hiroyasu Hasumi (Eds.)*

178 **Magma to Microbe: Modeling Hydrothermal Processes at Oceanic Spreading Centers** *Robert P. Lowell, Jeffrey S. Seewald, Anna Metaxas, and Michael R. Perfit (Eds.)*

179 **Active Tectonics and Seismic Potential of Alaska** *Jeffrey T. Freymueller, Peter J. Haeussler, Robert L. Wesson, and Göran Ekström (Eds.)*

180 **Arctic Sea Ice Decline: Observations, Projections, Mechanisms, and Implications** *Eric T. DeWeaver, Cecilia M. Bitz, and L.-Bruno Tremblay (Eds.)*

181 **Midlatitude Ionospheric Dynamics and Disturbances** *Paul M. Kintner, Jr., Anthea J. Coster, Tim Fuller-Rowell, Anthony J. Mannucci, Michael Mendillo, and Roderick Heelis (Eds.)*

182 **The Stromboli Volcano: An Integrated Study of the 2002–2003 Eruption** *Sonia Calvari, Salvatore Inguaggiato, Giuseppe Puglisi, Maurizio Ripepe, and Mauro Rosi (Eds.)*

183 **Carbon Sequestration and its Role in the Global Carbon Cycle** *Brian J. McPherson and Eric T. Sundquist (Eds.)*

184 **Carbon Cycling in Northern Peatlands** *Andrew J. Baird, Lisa R. Belyea, Xavier Comas, A. S. Reeve, and Lee D. Slater (Eds.)*

Geophysical Monograph 185

Indian Ocean Biogeochemical Processes and Ecological Variability

Jerry D. Wiggert
Raleigh R. Hood
S. Wajih A. Naqvi
Kenneth H. Brink
Sharon L. Smith
Editors

American Geophysical Union
Washington, DC

Published under the aegis of the AGU Books Board

Kenneth R. Minschwaner, Chair; Gray E. Bebout, Joseph E. Borovsky, Kenneth H. Brink, Ralf R. Haese, Robert B. Jackson, W. Berry Lyons, Thomas Nicholson, Andrew Nyblade, Nancy N. Rabalais, A. Surjalal Sharma, Darrell Strobel, Chunzai Wang, and Paul David Williams, members.

Library of Congress Cataloging-in-Publication Data

Indian ocean biogeochemical processes and ecological variability / Jerry D. Wiggert [... et al.], editors.

p. cm. — (Geophysical monograph series ; v.185) 1. Chemical oceanography—Indian Ocean. 2. Marine chemical ecology—Indian Ocean. 3. Carbon cycle (Biogeochemistry)—Indian Ocean. 4. Monsoons—Indian Ocean. 5. Indian Ocean—Environmental conditions. I. Wiggert, Jerry D., 1963-

GC721.I493 2009

551.46′615—dc22

2009040312

ISBN: 978-0-87590-475-7

ISSN: 0065-8448

Cover Image: Ocean chlorophyll measurements from Aqua-MODIS covering the period from 21 September 2006 through 20 December 2006. These reveal the anomalous biological distributions that occur, particularly off the south (west) coast of Java (Sumatra), under the influence of the Indian Ocean dipole. Image created by Norman Kuring from data processed by the Ocean Biology Processing Group at NASA's Goddard Space Flight Center (http://oceancolor.gsfc.nasa.gov/) and from the Earth Observatory's "Blue Marble: Next Generation" data set (http://earthobservatory.nasa.gov/Features/BlueMarble/bmng.pdf).

CONTENTS

PREFACE

Although there have been significant advances in our ability to describe and model the oceanic environment, our understanding of the physical, biogeochemical, and ecological dynamics of the Indian Ocean is still rudimentary in many respects. This is partly because the Indian Ocean remains substantially under sampled, in both space and time, compared to the Atlantic and Pacific oceans. The situation is compounded by the Indian Ocean being a dynamically complex and highly variable system under monsoonal influence. The biogeochemical and ecological impacts of this complex physical forcing are not yet fully understood. The Indian Ocean is truly one of the last great frontiers of oceanographic research. In addition, it appears to be particularly vulnerable to climate change and anthropogenic impacts, yet it has been more than a decade since the last coordinated international study of biogeochemical and ecological processes was undertaken in this region. To obtain a better understanding of the atmospheric and oceanic variability in the Indian Ocean, the Climate Variability and Predictability program (CLIVAR) and the Global Ocean Observing System (GOOS) are deploying a basin-wide observing system in the Indian Ocean. As well, several nations are deploying coastal observing systems. These, in combination with newly available research capabilities and technologies, provide a unique opportunity for staging international, interdisciplinary research in the Indian Ocean.

The chapters in this volume are derived from an international conference that was convened in Goa, India, 3–6 October 2006. Major funding for this event was provided by the National Science Foundation (NSF grant OISE-0536861) and India's National Institute of Oceanography (Council of Scientific and Industrial Research), with additional contributions provided by several other agencies and Indian Ocean rim nations. The goal of this conference was to assess the current state of our knowledge of the biogeochemical and ecosystem dynamics of the Indian Ocean, with a view toward initiating a new international research program. This initiative (Sustained Indian Ocean Biogeochemistry and Ecosystem Research or SIBER) has been formally approved and is now sponsored by the Integrated Marine Biogeochemistry and Ecosystem Research (IMBER) program and the Indian Ocean Global Ocean Observing System (IOGOOS). SIBER, which also maintains close ties to the CLIVAR Indian Ocean Panel, is a basin-wide effort that has worked to identify the major scientific questions needing attention in the Indian Ocean and has developed an overarching plan for addressing them. We believe that SIBER is the beginning of a new era of collaborative, interdisciplinary (physical, biogeochemical, and ecological) research in the Indian Ocean. We thank all of the authors who have contributed to this monograph as well as all conference participants for their enthusiastic support, participation, and input that led to the publication of this volume and the development of the SIBER program.

Raleigh R. Hood
University of Maryland Center for Environmental Science

S. Wajih A. Naqvi
National Institute of Oceanography

Jerry D. Wiggert
University of Southern Mississippi

Indian Ocean Biogeochemical Processes and Ecological Variability
Geophysical Monograph Series 185

10.1029/2009GM000907

Introduction to Indian Ocean Biogeochemical Processes and Ecological Variability: Current Understanding and Emerging Perspectives

Jerry D. Wiggert,[1] Raleigh R. Hood,[2] S. Wajih A. Naqvi,[3]
Kenneth H. Brink,[4] and Sharon L. Smith[5]

Despite a history of exploration dating back to the classical era and its leading role as a pathway for trade and cultural exchange for the great civilizations of those times, the Indian Ocean has consistently been subject to less attention in the modern era in terms of oceanographic enquiry. The cornerstone of the Sustained Indian Ocean Biogeochemical and Ecosystem Research (SIBER) initiative has been to promote more frequent and persistent research activities that encompass the entire Indian Ocean basin and to facilitate international cooperation to realize these objectives. This volume's chapters are derived from the plenary talks given by the attendees of the first SIBER conference and are a blend of current knowledge reviews and new results. Thus this collection of papers represents an interdisciplinary contribution to the Indian Ocean literature by the leading members of the Indian Ocean research community.

During the classical period, India was a trading hub that promoted broad cross-cultural exchanges between the Mediterranean world of the Greek city-states and the Roman Empire to the west and Asian civilizations in Indonesia and China to the east. Indeed, archaeological evidence (wine amphorae, Roman coins, glass, and tableware) indicates that significant trading activity took place between Rome and sites situated from Cochin around the peninsula to Arikamedu, with sea trade reaching 120 ships annually during the reign of Augustus (31 B.C. to 14 A.D.) [*Boorstin*, 1991; *Keay*, 2000]. Moreover, the widespread export of Buddhism to the Far East profoundly affected the evolution of those societies. These far-reaching economic and cultural exchanges were fundamentally enabled by the semiannually reversing monsoon winds that simplified navigation across the Arabian Sea and were well known to the Greek and Egyptian sailors of that era. Indeed, the SW monsoon was once termed the Hippalus after the Greek pilot who first discovered how to navigate from the Red Sea to the Indian ports along the Konkan and Malabar coasts [*Boorstin*, 1991].

From the early seventh century, Chinese traders were regularly engaged in seagoing commerce with merchants in Kozhikode (Calicut). By the early fifteenth century, Chinese mariners had already mapped much of the Indian Ocean's terrestrial boundaries, including the entire east African coast, with exemplary accuracy [*Menzies*, 2004]. Thus through the early history of the primary seafaring nations, and well into late antiquity, the Indian Ocean was by far the best known and frequently traveled of the world's oceans. It is indeed ironic that the seafaring European powers' search

[1]Department of Marine Sciences, University of Southern Mississippi, Stennis Space Center, Mississippi, USA.
[2]Horn Point Laboratory, University of Maryland Center for Environmental Science, Cambridge, Maryland, USA.
[3]National Institute of Oceanography, Council of Scientific and Industrial Research, Dona Paula, India.
[4]Woods Hole Oceanographic Institution, Woods Hole, Massachusetts, USA.
[5]Rosenstiel School of Marine and Atmospheric Science, University of Miami, Miami, Florida, USA.

Indian Ocean Biogeochemical Processes and Ecological Variability
Geophysical Monograph Series 185

10.1029/2009GM000906

for a more direct route to South/Southeast Asia's tantalizing spices (black pepper, cinnamon, nutmeg, and cloves) in the late fifteenth century would lead to the diminishment in economic focus and geopolitical role of the Indian Ocean relative to the other ocean basins. This focal point shift has fundamentally contributed to retarding the pace of advances in our scientific understanding of the Indian Ocean.

The ship tracks of the HMS *Beagle* (1831–1836) and the HMS *Challenger* (1872–1876) are clearly symptomatic of this shift in focus. The *Beagle*'s course between King George's Sound and Cape Town ventured only as far north as the Cocos (Keeling) Islands (~12°S) in the southeastern Indian Ocean, while the *Challenger* Expedition's course between Cape Town and Melbourne lay primarily in the Indian sector of the Southern Ocean with the two port calls marking its northern limits. The field of oceanography is considered to have been initiated with the *Challenger* Expedition's voyage, and in the subsequent years into the early twentieth century, numerous permanent stations for the study of marine science were established [*Sverdrup et al.*, 1957]. However, with the exception of the mostly biological work carried out around British India by the "Surgeon-Naturalists" on board the RIMS *Investigator I* and RIMS *Investigator II* between 1881 and 1926 using some of the *Challenger*'s gear [*Qasim,* 1998], it was not until the John Murray Expedition (1933–1934) to the Arabian Sea, on the Egyptian research vessel *Mabahiss*, that the Indian Ocean proper was the target of a major oceanographic survey (a summary of the expedition's principal findings is given by *Wiggert et al.* [2005]).

The next major oceanographic initiative to occur was the International Indian Ocean Expedition (IIOE) (1960–1965), which was organized by the Special (later Scientific) Committee on Oceanographic Research. During the formative stages of the IIOE, a newsletter entitled "*The Indian Ocean Bubble*" was published and distributed anonymously. Its purpose was to act as an informal medium for exchanging views, ideas, and communications that would help identify just what an internationally organized expedition to the Indian Ocean "would like to try to do." The originator of this newsletter was later revealed to be Henry Stommel [*Hogg and Huang*, 1995]. Over its five-issue run, several of the expressed views can be seen as having long-standing implications for future activities in the basin. In particular, the salinity heterogeneity in the Bay of Bengal was seen as a troublesome interpretive aspect so the recommendation to focus on the Arabian Sea for studying the monsoonal current reversals was made. The seasonality of the equatorial currents was also an open question, since zonal wind stress over the tropical Indian Ocean is unique in comparison with the Pacific and Atlantic oceans, so investigating this dynamic process was identified as a priority. A third prominent view expressed within the *Indian Ocean Bubble*'s communications was the crucial need for establishment of a regional institution that could take on the data assembly and analysis needs of the IIOE activities and that would subsequently develop into a permanent facility that enabled regionally administered oceanographic studies in the Indian Ocean. This vision of the contributors to "The Bubble" was prominently realized through establishment of the National Institute of Oceanography in Goa, India, in 1966; it also helped to facilitate the promotion and development of the marine science programs of Pakistan, Thailand, and Indonesia [*Wooster*, 1984].

While the IIOE was principally geared toward addressing basic gaps in the understanding of the Indian Ocean's complement of unique dynamical processes, biological measurements were also performed. These ultimately led to creation of several plankton and production atlases [e.g., *Indian Ocean Biological Center*, 1968; *Panikkar*, 1970; *Krey and Babenerd*, 1976; *Qasim*, 1978] that, into the 1980s, essentially represented the state of our knowledge of these faunal distributions. This is a clear testament to the breadth of the IIOE; yet it also is a telling indicator of the level of international participation in Indian Ocean studies relative to that afforded to the other ocean basins. Summaries of research efforts focused on illuminating biogeochemical processes in the Indian Ocean leading up to and including the Joint Global Ocean Flux Study (JGOFS) campaigns have been developed elsewhere [see *Wiggert et al.*, 2005; *Hood et al.*, this volume] and will not be reiterated here, except to stress that the bulk of these activities have occurred in the Arabian Sea. Thus a principle need going forward is for such research efforts to be inclusive of the entire Indian Ocean. Indeed, this is a principal tenet of the conceptual framework that underlies the Sustained Indian Ocean Biogeochemical and Ecosystem Research (SIBER) initiative.

SIBER's initial development and underlying motivations are discussed in the monograph's preface, while current and emerging fundamental scientific questions, as well as near-future potential for leveraging ongoing observing system infrastructure expansion, are discussed in the closing chapter by *Hood et al.* [this volume]. The intervening chapters are a mixture of overview articles that summarize the current state of knowledge for a given topic and reports on new research results or some integrated combination of both perspectives. All of the chapters are derived from the set of invited plenary talks that were presented at the initial SIBER workshop held at the National Institute of Oceanography (NIO) in Goa in October 2006. The chapter ordering progresses through papers that discuss (1) the overlying physical processes set by monsoonal forcing and how these control biological production and variability; (2) nutrient cycling and limitation;

(3) pelagic carbon cycling and air-sea exchange; (4) benthic biogeochemistry and ecology; and (5) the impact of climate and human activities on biogeochemistry and ecosystems. Thus this ordering reflects an overall transition downward through the water column and toward broader scales of spatiotemporal variability that integrate climate and anthropogenic impacts. As indicated above, these contributions range from syntheses of mature research directions to newly emerging tacks, and they employ the full gamut of oceanographic methods that include classical ship-based activities, long-term deployed instrument arrays and observing systems, remote sensing data streams, and coupled physical-biogeochemical models.

Biological variability in the Indian Ocean is fundamentally linked to the basin's monsoonal forcing that drives semiannual upwelling events, wintertime convective mixing (Arabian Sea), and current reversals down to ~10°S. The basin-wide evolution of physical-biological processes that results from the monsoon winds is reviewed by *McCreary et al*. [this volume], as are processes at intraseasonal and interannual time scales. The mechanisms that contribute to the contrast in production magnitude that occurs between the Arabian Sea and Bay of Bengal, despite similar monsoonal wind forcing, are explored by *Prasanna Kumar et al*. [this volume]. Identifying interregional contrasts in bloom dynamics and exploring how these seasonally evolve is also the focal point of the chapter by *Marra and Moore* [this volume], where monsoon-impacted phytoplankton distributions from the Arabian Sea, Indonesian Seas, and West Australian shelf are featured. The focus on the two latter regions brings into consideration the effect of the Indonesian Throughflow on Indian Ocean biological processes, a poorly represented topic in the oceanographic literature. The large-magnitude river inflows of the Bay of Bengal exert prominent hydrologic controls on the bay's ecosystem; the impact of this control, in conjunction with monsoon forcing, coastal currents, cyclones, and mesoscale eddies, is characterized by *Vinayachandran* [this volume] using remotely sensed chlorophyll distributions.

A thorough exploration of historical hydrographic observations from the northern Arabian Sea, which included a considerable effort in data mining, has been performed by *Banse and Postel* [this volume], who report on the nature of a previously unidentified water mass that forms poleward of 21°–22°N through the active evaporation of the winter monsoon that they name "North Arabian Sea High Salinity Water." In their chapter on abundances of bacterioplankton, *Ramaiah et al*. [this volume] report on distributional contrasts in the seasonal variation of bacterial production rates observed between the Arabian Sea and Bay of Bengal that exhibit monsoonal impacts, as well as the essentially constant rates observed in equatorial waters. The final contribution to the group of papers focusing on production is provided by *Landry* [this volume], who reprises several divergent interpretations of zooplankton observations obtained during the JGOFS cruises of the mid-1990s through the use of a food web synthesis that elucidates how mesozooplankton and microzooplankton contribute to carbon flows within the Arabian Sea ecosystem.

Of the papers that focus on nutrient cycling and nutrient limitation patterns in the Indian Ocean, the first contribution is by *Koné et al*. [this volume]. They report on how well their coupled physical-biogeochemical model simulates the observed distribution and timings of the basin's bloom dynamics and how these blooms are controlled by various physical processes and/or evolution of nutrients most limiting to primary production (N, Fe, or Si). The remaining contributions in this group of papers focus on nitrogen (N) cycling. *Mulholland and Capone* [this volume] review the current state of knowledge of diazotrophy in the Indian Ocean and primarily conclude that a diverse assemblage of diazotrophs is present and that it is likely that processes such as the monsoon cycle, riverine input, and atmospheric deposition all contribute to spatiotemporal variability in dinitrogen fixation. However, as yet, insufficient data are available to illuminate this inference. The Arabian Sea's oxygen minimum zone (OMZ) is well known as one of the three prominent open ocean sites where loss of fixed nitrogen occurs, though whether to ascribe this to anammox or denitrification has been unclear. Through use of gene expression techniques, *Jayakumar et al*. [this volume] have explored the relative contributions of these processes in the Arabian Sea's OMZ and found that denitrifier assemblages are numerically dominant and appear to exhibit a more dynamic response to environmental variability. The final N cycling paper is provided by *Bange* [this volume], who reviews the current state of understanding regarding the production of nitrous oxide (N_2O), a notable greenhouse gas, the production of which is stimulated by oxygen deficiency in the water column.

The first paper from the group focusing on carbon cycling and air-sea exchange is from *Hansell* [this volume], who reports on a model-derived distribution of surface dissolved organic carbon (DOC) that is validated with measurements from several regions of the Indian Ocean. The more extensive Arabian Sea data set provides the means to assess the seasonality of net DOC production and consumption indicated by the model. The contribution by *Goyet and Touratier* [this volume] reports on their application of a method for estimating penetration of anthropogenic CO_2 into the Indian Ocean. Their results reveal a sharp contrast between the Arabian Sea and Bay of Bengal, suggesting deep penetration of the anthropogenic signal in the southern Indian Ocean,

and generally underscore the urgent need for understanding how ocean acidification will unfold in the Indian Ocean. Focusing on the contrasts in, and associated controls of, net community production (NCP) in the Arabian Sea and the Bay of Bengal, *Sarma* [this volume] provides a review of the current understanding, with comparison to other recent analyses. In the Arabian Sea, net autotrophy is established during the summer monsoon and the eastern (western) areas are predominantly heterotrophic (autotrophic). In contrast, the increased river inputs of the summer monsoon drive the Bay of Bengal toward heterotrophy, while contrary to other analyses, it was concluded that enhanced export of particulate matter in river discharge does not promote removal of atmospheric CO_2. A synthesis of the organic matter quality of export fluxes measured at sites from the Arabian Sea to the Java coast is contributed by *Unger and Jennerjahn* [this volume], who find that because of a highly variable contribution of foraminifera to carbonate the Indian Ocean does not exhibit the strong correlation of particulate organic carbon to carbonate fluxes typical of the world's oceans. Moreover, regional differences in bacterial production in the northern Indian Ocean result from differences in food web structure, where zooplankton are more prominent in the Arabian Sea, while bacterial biomass is promoted in the Bay of Bengal by the substantial river inputs. Further study is advocated to assess how these divergent food web structures affect regional export efficiency.

Anderson and Ryabchenko [this volume] close out the contributions on carbon cycling with their chapter that reports on a model focusing on the central Arabian Sea that examines the organic matter flows that fuel bacterial production. They conclude that local sources of organic material are insufficient, thus promoting the argument that advective input is necessary to maintain the observed production rates. The overall collection of contributions that cover elemental cycling is completed by two chapters that focus on how these processes are affected by the OMZ waters of the eastern Arabian Sea's continental margin. In the data synthesis of *Law et al*. [this volume], measurements from waters on the Pakistan margin were used to characterize the aerobic and anaerobic contributions to microbially mediated C oxidation. Using data from locations that ranged from oxygenated to seasonally hypoxic to fully anoxic, they found that reduction rates were as much as 85% lower in OMZ waters. In a synthesis of sedimentary $\delta^{15}N$ records from locations where coastal upwelling or anthropogenic alterations affect coastal hypoxia, *Agnihotri et al*. [this volume] conclude that the west Indian shelf is subject to both climate-related intensified upwelling and human-induced eutrophication. Furthermore, while sedimentary $\delta^{15}N$ is typically seen to increase over the Anthropocene because of both influences, this is not apparent in the eastern Arabian Sea; this leads the authors to reconsider the utility of sedimentary $\delta^{15}N$ as a denitrification proxy in coastal waters.

The final set of chapters consists of contributions that highlight how climate and anthropogenically induced change has been observed to influence ecological and biogeochemical processes in the Indian Ocean. The first in this group is a synthesis by *Naqvi et al*. [this volume] that provides a long-term characterization of water quality in the eastern Arabian Sea. They report that annually recurring subsurface hypoxia associated with upwelling of high-nutrient, low-oxygen waters along the west Indian shelf during the summer monsoon appears to be subject to interannual variability and decadal intensification. Increased rates of aeolian nitrogen deposition are identified as the primary nutrient-loading mechanism behind the overall eutrophication, while interannual variation is attributed to the physical environment, which may be modulated by broader-scale climate signals. A recently appearing transition in phytoplankton speciation is documented in the chapter by *Gomes et al*. [this volume], who have identified a shift from diatoms to a large dinoflagellate (*Noctiluca miliaris*) during the winter monsoon's typical bloom period in the northern Arabian Sea. The intensifying concentrations of *N. miliaris* within these winter blooms directly contrasts its meager standing within the species complement of samples obtained during the JGOFS cruises of the 1990s as well as those from the IIOE cruises of the early 1960s.

Both monsoon and climate impacts on particle flux are considered by *Rixen et al*. [this volume] in their chapter that synthesizes sediment trap data from several regions of the Indian Ocean to assess the biological pump's response to these influences. They report that in the Arabian Sea upwelling system the biological pump is bottom-up controlled and sensitive to iron supply and, in general, weaker than in the freshwater-influenced continental margins of the eastern Indian Ocean. Further, the El Niño–Southern Oscillation–linked influence on interannual variability in summertime precipitation and associated river inflows in these eastern regions leads to enhanced (reduced) oceanic CO_2 outgassing during El Niño (La Niña). The influence of the positive phase of the Indian Ocean dipole (IOD) on surface chlorophyll distributions and a first assessment of the associated modification of basin-wide primary production is provided by *Wiggert et al.* [this volume] through utilization of the 10+ years of Sea-viewing Wide Field-of-view Sensor (SeaWiFS) ocean color data. While the influence of the IOD on spatiotemporal biological variability is clear, the carbon uptake rates obtained through application of a net production algorithm indicate a zero-sum impact when integrated over the full Indian Ocean basin. Nevertheless, a fundamental reorganization of biogeochemical fluxes occurs during IOD periods, which points to

a crucial need for sustained observations at key locations so that quantification of the modified uptake and export flux distributions can be obtained.

The last chapter in this collection is provided by *Hood et al*. [this volume], who summarize past oceanographic research activities in the basin and the conclusions of the first SIBER workshop, which was the genesis for all of the chapters herein. Within their synopsis of the SIBER workshop findings they highlight several key, and recently emerging, questions including the relative role of iron limitation and zooplankton grazing pressure for controlling phytoplankton growth in the Arabian Sea; the manifest uncertainties that exist in current rate estimates of dinitrogen fixation and denitrification, though both are clearly prominent; and the need for establishing current baselines for all aspects of biogeochemical cycling so that the continual and expanding influence of global climate change and anthropogenic influences associated with the exploding human populations and accompanying land use changes bordering the Indian Ocean can be recognized and accurately quantified.

It is fair to say that the collection of works within this monograph represent an interdisciplinary contribution to the Indian Ocean literature that has no recent or previous counterpart of similar scope, particularly in terms of promoting the adoption of a holistic approach to oceanographic research in this basin. With the ongoing deployment of the Research Moored Array for African-Asian-Australian Monsoon Analysis and Prediction (RAMA) array throughout the Indian Ocean [*McPhaden et al.*, 2009] and our expanding understanding of linkages between monsoon variability and the southern tropical regions of the Indian Ocean [*Izumo et al.*, 2008; *Vialard et al.*, 2009], opportunities for a concomitant expansion of biogeochemical research to more remote locations is a clear necessity and should materialize with greater frequency. The global coverage afforded by remote sensing platforms, in particular the ongoing extension of ocean color-based capabilities, should also motivate more active programs of sampling in heretofore poorly characterized regions; indeed, the recent unveiling of an ocean color algorithm that utilizes the additional chlorophyll-fluorescence band deployed on the Moderate Resolution Imaging Spectroradiometer (MODIS) to identify regions prone to iron stress suggests that a broad swath of iron limitation develops seasonally in the southern Indian Ocean [*Behrenfeld et al.*, 2009]. This finding agrees well with the distributions predicted by a coupled physical-biogeochemical model [*Wiggert et al.*, 2006]. In addition to forward looking adoption of new techniques, such as the gene expression methods detailed in the chapter by *Jayakumar et al*. [this volume; see also *Ward*, 2005; *Jayakumar et al.*, 2009], the chapter by Banse and Postel underscores the utility of data mining and the need to retain, and make broadly available, observations from past research campaigns. In this vein, the release by NIO of a pair of data CDs that are a compendium of past physical and biological observations by the institution's oceanographers is heartening to see (http://www.nio.org/iodc/cds.php). Efforts to generate and make available such informational resources will hopefully continue and should be encouraged.

In closing, the syntheses and new results presented in these chapters provide a wealth of past knowledge, new insight into long-standing research questions, and a host of implications and emerging questions. These should serve to motivate fruitful inquiries for both the established scientists that have contributed to this volume and for the young and energetic scientists who also acquire the passion to delve into the unique nature of the Indian Ocean.

Acknowledgments. The authors would like to thank Karl Banse for pointing out the exchanges of Henry Stommel and colleagues that appeared in "The Indian Ocean Bubble" as they considered research priorities for the then upcoming IIOE campaign. Major funding for the first SIBER workshop was provided by the National Science Foundation (NSF grant OISE-0536861) and India's National Institute of Oceanography (Council of Scientific and Industrial Research), with additional contributions provided by several other agencies and Indian Ocean rim nations.

REFERENCES

Agnihotri, R., S. W. A. Naqvi, S. Kurian, M. A. Altabet, and J. F. Bratton (2009), Is $\delta^{15}N$ of sedimentary organic matter a good proxy for paleodenitrification in coastal waters of the eastern Arabian Sea?, *Geophys. Monogr. Ser.*, doi:10.1029/2008GM000770, this volume.

Anderson, T. R., and V. A. Ryabchenko (2009), Carbon cycling in the mesopelagic zone of the central Arabian Sea: Results from a simple model, *Geophys. Monogr. Ser.*, doi:10.1029/2007GM000686, this volume.

Bange, H. W. (2009), Nitrous oxide in the Indian Ocean, *Geophys. Monogr. Ser.*, doi:10.1029/2008GM000762, this volume.

Banse, K., and J. R. Postel (2009), Wintertime convection and ventilation of the upper pycnocline in the northernmost Arabian Sea, *Geophys. Monogr. Ser.*, doi:10.1029/2008GM000704, this volume.

Behrenfeld, M. J., et al. (2009), Satellite-detected fluorescence reveals global physiology of ocean phytoplankton, *Biogeoscience*, *6*, 779–794.

Boorstin, D. J. (1991), *The Discoverers: An Illustrated History of Man's Search to Know His World and Himself*, 1024 pp., Abrams, New York.

Gomes, H. do R., S. G. Prabhu Matondkar, S. G. Parab, J. I. Goes, S. Pednekar, A. R. N. Al-Azri, and P. G. Thoppil (2009), Unusual blooms of the green *Noctiluca miliaris* (Dinophyceae) in the Arabian Sea during the winter monsoon, *Geophys. Monogr. Ser.*, doi:10.1029/2008GM000831, this volume.

Goyet, C., and F. Touratier (2009), Challenges for present and future estimates of anthropogenic carbon in the Indian Ocean, *Geophys. Monogr. Ser.*, doi:10.1029/2008GM000754, this volume.

Hansell, D. A. (2009), Dissolved organic carbon in the carbon cycle of the Indian Ocean, *Geophys. Monogr. Ser.*, doi:10.1029/2007GM000684, this volume.

Hogg, N. G., and R. X. Huang (Eds.) (1995), *Collected Works of Henry M. Stommel*, 380 pp., Am. Meteorol. Soc., Boston, Mass.

Hood, R. R., J. D. Wiggert, and S. W. A. Naqvi (2009), Indian Ocean research: Opportunities and challenges, *Geophys. Monogr. Ser.*, doi:10.1029/2008GM000714, this volume.

Indian Ocean Biological Center (1968), *Maps on Total Zooplankton Biomass in the Arabian Sea and the Bay of Bengal*, vol. I, fasc. 1, Natl. Inst. of Oceanogr., New Delhi.

Izumo, T., C. de Boyer Montegut, J.-J. Luo, S. K. Behera, S. Masson, and T. Yamagata (2008), The role of the western Arabian Sea upwelling in Indian monsoon rainfall variability, *J. Clim.*, *21*, 5603–5623, doi: 10.1175/2008JCLI2158.1.

Jayakumar, A., W. W. A. Naqvi, and B. B. Ward (2009), Distribution and relative quantification of key genes involved in fixed nitrogen loss from the Arabian Sea oxygen minimum zone, *Geophys. Monogr. Ser.*, doi:10.1029/2008GM000730, this volume.

Jayakumar, A., G. D. O'Mullan, S. W. A. Naqvi, and B. B. Ward (2009), Denitrifying bacterial community composition changes associated with stages of denitrification in oxygen minimum zones, *Microb. Ecol.*, *58*, 350–362, 10.1007/s00248-009-9487-y.

Keay, J. (2000), *India: A History*, 576 pp., Grove, New York.

Koné, V., O. Aumont, M. Lévy, and L. Resplandy (2009), Physical and biogeochemical controls of the phytoplankton seasonal cycle in the Indian Ocean: A modeling study, *Geophys. Monogr. Ser.*, doi:10.1029/2008GM000700, this volume.

Krey, J., and B. Babenerd (1976), *Phytoplankton Production: Atlas of the International Indian Ocean Expedition*, 70 pp., Inst. für Meeresk., Kiel Univ., Kiel, Germany.

Landry, M. R. (2009), Grazing processes and secondary production in the Arabian Sea: A simple food web synthesis with measurement constraints, *Geophys. Monogr. Ser.*, doi:10.1029/2008GM000781, this volume.

Law, G. T. W., G. L. Cowie, E. R. Breuer, M. C. Schwartz, S. M. Harvey, C. Woulds, T. M. Shimmield, G. B. Shimmield, and K. A. Doig (2009), Rates and regulation of microbially mediated aerobic and anaerobic carbon oxidation reactions in continental margin sediments from the northeastern Arabian Sea (Pakistan margin), *Geophys. Monogr. Ser.*, doi:10.1029/2008GM000765, this volume.

Marra, J., and T. S. Moore II (2009), Monsoons, islands, and eddies: Their effects on phytoplankton in the Indian Ocean, *Geophys. Monogr. Ser.*, doi:10.1029/2008GM000701, this volume.

McCreary, J. P., R. Murtugudde, J. Vialard, P. N. Vinayachandran, J. D. Wiggert, R. R. Hood, D. Shankar, and S. Shetye (2009), Biophysical processes in the Indian Ocean, *Geophys. Monogr. Ser.*, doi:10.1029/2008GM000768, this volume.

McPhaden, M. J., G. Meyers, K. Ando, Y. Masumoto, V. S. N. Murty, M. Ravichandran, F. Syamsudin, J. Vialard, L. Yu, and W. Yu (2009), RAMA: The Research Moored Array for African-Asian-Australian Monsoon Analysis and Prediction, *Bull. Am. Meteorol. Soc.*, *90*, 459–480.

Menzies, G. (2004), *1421: The Year China Discovered America*, HarperCollins, New York.

Mulholland, M. R., and D. G. Capone (2009), Dinitrogen fixation in the Indian Ocean, *Geophys. Monogr. Ser.*, doi:10.1029/2009GM000850, this volume.

Naqvi, S. W. A., H. Naik, D. A. Jayakumar, A. K. Pratihary, G. Narvenkar, S. Kurian, R. Agnihotri, M. S. Shailaja, and P. V. Narvekar (2009), Seasonal anoxia over the western Indian continental shelf, *Geophys. Monogr. Ser.*, doi:10.1029/2008GM000745, this volume.

Panikkar, N. K. (Ed.) (1970), *International Indian Ocean Expedition Plankton Atlas: Distribution of Fish Eggs and Larvae in the Indian Ocean*, Indian Ocean Biol. Cent., Panaji, India.

Prasanna Kumar, S., J. Narvekar, M. Nuncio, M. Gauns, and S. Sardesai (2009), What drives the biological productivity of the northern Indian Ocean?, *Geophys. Monogr. Ser.*, doi:10.1029/2008GM000757, this volume.

Qasim, S. Z. (1978), Distribution of chlorophyll a in the Indian Ocean, *Indian J. Mar. Sci.*, *7*, 258–262.

Qasim, S. Z. (1998), *Glimpses of the Indian Ocean*, 224 pp., Universities Press, Hyderabad, India.

Ramaiah, N., V. Fernandes, V. V. Rodrigues, J. T. Paul, and M. Gauns (2009), Bacterioplankton abundance and production in Indian Ocean regions, *Geophys. Monogr. Ser.*, doi:10.1029/2008GM000711, this volume.

Rixen, T., V. Ramaswamy, B. Gaye, B. Herunadi, E. Maier-Reimer, H. W. Bange, and V. Ittekkot (2009), Monsoonal and ENSO impacts on particle fluxes and the biological pump in the Indian Ocean, *Geophys. Monogr. Ser.*, doi:10.1029/2008GM000706, this volume.

Sarma, V. V. S. S. (2009), Net community production in the northern Indian Ocean, *Geophys. Monogr. Ser.*, doi:10.1029/2008GM000715, this volume.

Sverdrup, H. U., M. W. Johnson, and R. H. Fleming (1957), *The Oceans: Their Physics, Chemistry and General Biology*, 7th ed., 1087 pp., Prentice-Hall, Englewood Cliffs, N. J.

Unger, D., and T. Jennerjahn (2009), Impact of regional Indian Ocean characteristics on the biogeochemical variability of settling particles, *Geophys. Monogr. Ser.*, doi:10.1029/2008GM000703, this volume.

Vialard, J., et al. (2009), Cirene: Air-sea interactions in the Seychelles-Chagos thermocline ridge region, *Bull. Am. Meteorol. Soc.*, *90*, 45–61, 10.1175/2008BAMS2499.1.

Vinayachandran, P. N. (2009), Impact of physical processes on chlorophyll distribution in the Bay of Bengal, *Geophys. Monogr. Ser.*, doi:10.1029/2008GM000705, this volume

Ward, B. B. (2005), Molecular approaches to marine microbial ecology and the marine nitrogen cycle, *Annu. Rev. Earth Planet. Sci.*, *33*, 301–333.

Wiggert, J. D., R. R. Hood, K. Banse, and J. C. Kindle (2005), Monsoon-driven biogeochemical processes in the Arabian Sea, *Prog. Ocean.*, *65*, 176–213.

Wiggert, J. D., R. G. Murtugudde, and J. R. Christian (2006), Annual ecosystem variability in the tropical Indian Ocean: Results of a coupled bio-physical ocean general circulation model, *Deep Sea Res., Part II*, *53*, 644–676.

Wiggert, J. D., J. Vialard, and M. J. Behrenfeld (2009), Basin-wide modification of dynamical and biogeochemical processes by the positive phase of the Indian Ocean dipole during the SeaWiFS era, *Geophys. Monogr. Ser.*, doi:10.1029/2008GM000776, this volume.

Wooster, W. S. (1984), International studies of the Indian Ocean, 1959–1965, *Deep Sea Res., Part I*, *31*, 589–597.

K. H. Brink, Woods Hole Oceanographic Institution, Woods Hole, MA 02543, USA.

R. R. Hood, Horn Point Laboratory, University of Maryland Center for Environmental Science, Cambridge, MD 21613, USA.

S. W. A. Naqvi, National Institute of Oceanography, Council of Scientific and Industrial Research, Dona Paula, Goa 403 004, India.

S. L. Smith, Rosenstiel School of Marine and Atmospheric Science, University of Miami, Miami, FL 33149, USA.

J. D. Wiggert, Department of Marine Sciences, University of Southern Mississippi, Stennis Space Center, MS 39529, USA. (jerry.wiggert@usm.edu)

Biophysical Processes in the Indian Ocean

J. P. McCreary,[1] R. Murtugudde,[2] J. Vialard,[3] P. N. Vinayachandran,[4]
J. D. Wiggert,[5] R. R. Hood,[6] D. Shankar,[7] and S. Shetye[7]

Basic physical processes that impact biological activity in the Indian Ocean (IO), namely, near-surface processes (upwelling, entrainment, detrainment, and advection) and subsurface circulations (shallow overturning cells and subthermocline currents), are reviewed. In the Arabian Sea, there are upwelling blooms during the southwest monsoon (SWM) along Somalia, Oman, and the west coast of India. In the central Arabian Sea, the overall SWM (northeast monsoon; NEM) blooms appear to be a series of entrainment (detrainment) blooms forced by intraseasonal winds. In the western Bay of Bengal, a prominent NEM bloom results from the entrainment of a preexisting deep chlorophyll maximum (DCM). South of Sri Lanka, the SWM bloom is caused by coastal upwelling and Ekman suction, and is swept into the Bay of Bengal by the Southwest Monsoon Current. In the tropical, South IO (5–20°S), there is a weak, surface bloom during boreal summer when new production is enhanced by nutrient entrainment; the surface bloom is even weaker (or absent) during boreal winter because the mixed layer is thinner, the thermocline is deeper, and hence, nutrient entrainment weaker. At intraseasonal timescales, blooms are associated with wind events and Rossby waves/eddies, and they can be generated by both new production and entrainment of a preexisting DCM. During the 1997/1998 El Niño–Southern Oscillation/IO zonal dipole event, there was an upwelling bloom near Sumatra/Java in fall 1997, a much deeper DCM and weaker surface bloom along 5–10°S in spring 1998, and a weaker bloom in the Arabian Sea during the SWM of 1998.

1. INTRODUCTION

1.1. Background

Indian Ocean (IO) circulations and phytoplankton distributions are very different from those in the other oceans, a consequence of the unique forcing by monsoon winds (Figure 1). There are seasonally reversing monsoon winds in the Arabian Sea, the Bay of Bengal, and extending to 10°S, with a stronger clockwise (weaker counterclockwise) circulation during the summer (winter). Typically, there are no easterly winds (trades) on the equator, and as a result there is little or

[1]International Pacific Research Center, University of Hawai'i, Honolulu, Hawai'i, USA.
[2]Earth System Science Interdisciplinary Center, University of Maryland, College Park, Maryland, USA.
[3]IRD, LOCEAN, Université Pierre et Marie Curie, Paris, France.
[4]Centre for Atmospheric and Oceanic Sciences, Indian Institute of Science, Bangalore, India.
[5]Department of Marine Sciences, University of Southern Mississippi, Stennis Space Center, Mississippi, USA.
[6]University of Maryland Center for Environmental Science, Cambridge, Maryland, USA.
[7]National Institute of Oceanography, Council of Scientific and Industrial Research, Dona Paula, India.

Indian Ocean Biogeochemical Processes and Ecological Variability
Geophysical Monograph Series 185

10.1029/2008GM000768

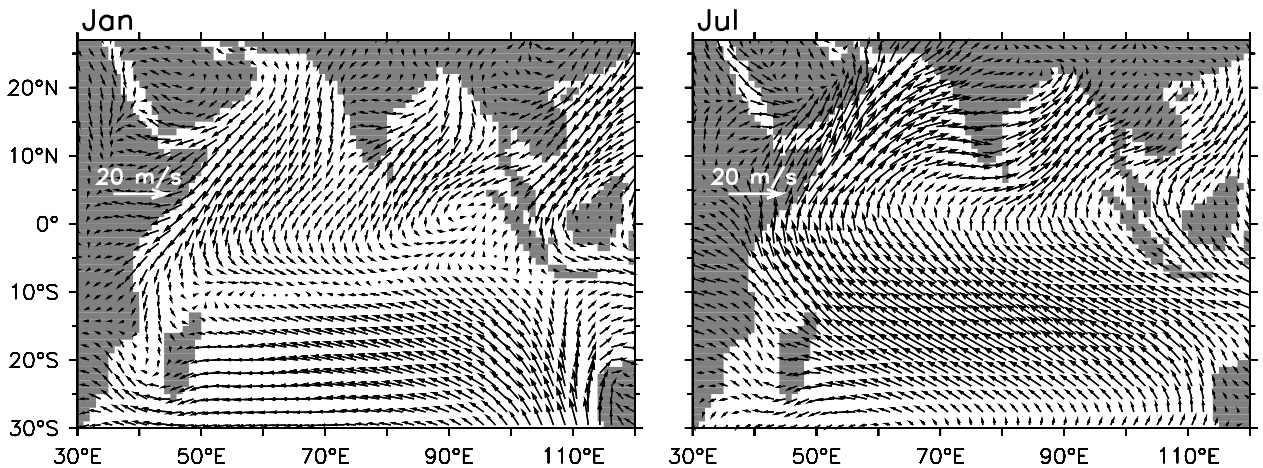

Figure 1. Maps of winds during (left) January and (right) July from an NCEP2 climatology averaged from 1979 to 2007.

no equatorial upwelling in the IO. (An exception occurs during IO zonal dipole mode (IOZDM) events (section 5) [*Wiggert et al.*, this volume]. The IOZDM is also referred to as the IO dipole (IOD), the IO zonal mode (IOZM), and the IO dipole zonal mode (IODZM).) South of 10°S, the southeast trades are relatively steady but stronger during austral winter.

Plate 1 (top) plots surface chlorophyll concentration, P, determined from a 1999–2007 climatology of Sea-viewing Wide Field-of-view Sensor (SeaWiFS) ocean-color data. To illustrate the ocean's response to the winds, Plate 1 (bottom) also plots the upper-layer thickness, h_1, from the model of *McCreary et al.* [1993] (hereinafter referred to as MKM); h_1 simulates the structure of the top of the actual thermocline reasonably well, except that it is somewhat too thin from 5 to 10°S. Note that there are regions where h_1 is thin enough to lie within the euphotic zone ($h_1 \lesssim 100$ m). These regions are biologically (and climatically) important either because upwelling is active or because anomalous forcings can thicken the mixed layer or raise the thermocline enough to allow subsurface (thermocline) waters, with their elevated nutrient concentrations, to be entrained into the surface layer. (In the MKM model, h_1 has a minimum allowed thickness of $H_m = 35$ m, so that upwelling is active in the solution almost everywhere where h_1 is shallower than the 40-m contour in Plate 1.) As discussed next, a comparison of the panels in Figure 1 and Plate 1 points toward close linkages among the wind forcing, h_1, and chlorophyll.

During July southwest monsoon (SWM), southwesterly winds blow along the Somali and Omani coasts and the east coast of India. These winds drive offshore Ekman drift, thinning h_1 along both coasts. The upwelling region along the east coast of India is less extensive and much weaker than that off Somalia and Oman. One reason for this difference is that the winds are considerably weaker in the Bay of Bengal. Another is that the region of thick h_1 in the eastern equatorial ocean (a Rossby-wave packet that reflected earlier from the eastern boundary of the basin) has a branch that spreads counterclockwise around the Bay (a coastal Kelvin wave); it overwhelms the upwelling along the northeast coast of India, so that h_1 actually thickens there, and thinning is confined to the southeast coast [*McCreary et al.*, 1996a; *Shankar et al.*, 1996; *Schott and McCreary*, 2001].

During July, there are also two, prominent regions of thin h_1 in the open ocean, one extending along 5–10°S and another south of Sri Lanka. Along 5–10°S, the overall thinning is generated by positive Ekman pumping velocity, w_{ek}, associated with the equatorward weakening of the southeast trades [MKM; *Yokoi et al.*, 2008; *Hermes and Reason*, 2008]. (The Ekman pumping velocity is related to the surface Ekman transport, $M_{ek} = (M^x, M^y) = (1/\rho_o)\,\hat{k} \times (\tau/f)$, where τ is the wind-stress vector, $\hat{k}$ is a unit vector in the z-direction, and f is the Coriolis parameter. Velocity w_{ek} is then the divergence of Ekman transport, that is, $w_{ek} = -\nabla \cdot M_{ek} = (1/\rho_o)\,\hat{k} \cdot \nabla \times (\tau/f)$. It is closely related to the wind-stress curl, but also includes effects due to the variability of f with latitude.) South of Sri Lanka, thermocline shoaling is partly driven by positive w_{ek} associated with the cyclonic bending of near-equatorial westerlies into the Bay during May and June. Later in the SWM, it is enhanced by remote forcing from the Bay of Bengal. Upwelling-favorable Kelvin waves, generated by the strong winds along the east coast of India, propagate around Sri Lanka and northward along the west

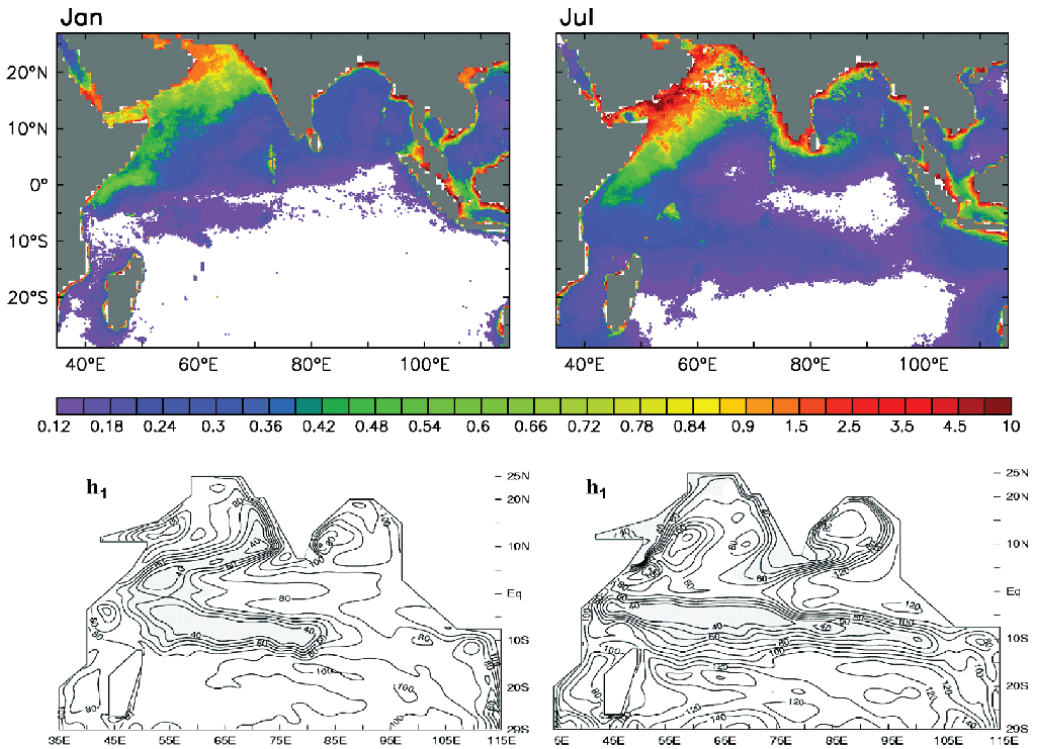

Plate 1. Maps of chlorophyll concentrations from (top) SeaWiFS and (bottom) thermocline depth h_1 from the model of *McCreary et al.* [1993; hereinafter MKM] during (left) January and (right) July. The chlorophyll plots are from a climatology averaged from September 1999 to August 2007. In the MKM model, h_1 has a minimum allowed thickness of H_m = 35 m, and upwelling of thermocline water into the mixed layer occurs in these regions (section 2.1). Bottom plots are reprinted from *McCreary et al.* [1993], with permission from Elsevier.

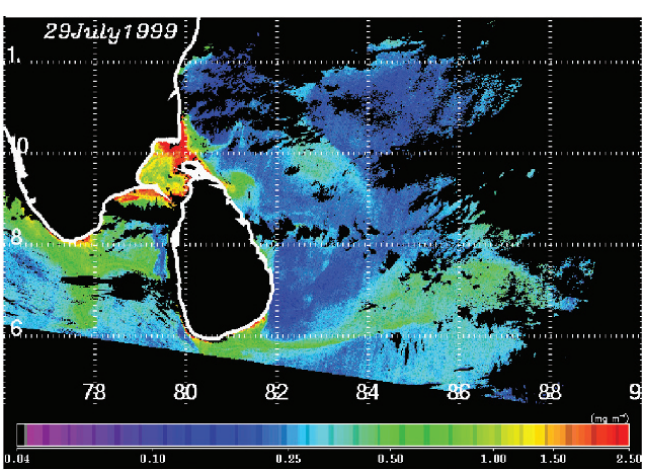

Plate 2. Phytoplankton concentrations from IRS-P4 OCM during July, 1999, illustrating the biophysical processes involved in the bloom south of Sri Lanka. After *Vinayachandran et al.* [2004].

coast of India; subsequently, this west-coast signal radiates into the interior of the Arabian Sea as a packet of Rossby waves, thinning h_1 well offshore (Plate 1, bottom right).

During January, near the peak of the northeast monsoon (NEM), h_1 is thick in the northern Arabian Sea, largely associated with convective mixing that is driven by northeasterly winds that carry cold, dry, continental air over the ocean (Plate 1, bottom left). Note that h_1 is also thick in the Bay of Bengal (lower right), contrary to observations; this error happens because the MKM model does not include effects of the large, summertime, freshwater flux into the Bay. In the real ocean, the fresh water generates a thin, stable, surface layer that remains throughout the winter. The h_1 field is thin in a band that extends across the southern Arabian Sea, the shallowing caused by an upwelling-favorable Rossby wave propagating from the west coast of India and by positive w_{ek} in the western basin. In the Southern Hemisphere, the 5–10°S ridge is confined to the western/central basin, a consequence of the weaker southeast trades during austral winter. The seasonal cycle of h_1, however, is more complex than suggested by the January and July snapshots in Plate 1. It has a prominent semiannual cycle driven by w_{ek} and is impacted by Rossby waves remotely generated in the eastern basin [*Yokoi et al.*, 2008; *Hermes and Reason*, 2008].

In the Northern Hemisphere, much of the July phytoplankton response is linked to upwelling regions where h_1 is shallow, with the strongest response occurring in the western Arabian Sea where the upwelling is most intense (Plate 1, right). At the same time, there is also a bloom in the central Arabian Sea where h_1 is *not* thin, which therefore is not a direct result of coastal upwelling (section 3.1). During January, there is a prominent bloom in the northern Arabian Sea, with weaker activity elsewhere; it also occurs in a region where climatological h_1 is thick and so is also not an upwelling bloom (Plate 1, left).

In the Southern Hemisphere, there are indications of a weak bloom along the 5–10°S thermocline ridge throughout the year (Plate 1, top). [The term "bloom" is commonly used to refer only to large-amplitude, episodic, phytoplankton events. Throughout this paper, we use the term more broadly, to apply if chlorophyll values are higher than background values (~0.05 mg/m^3) in a particular region regardless of timescale.] During austral winter (top right), the bloom forms a distinct band that extends across most of the basin from 5°S to 20°S. During austral summer (top left), however, it is confined primarily west of 75°E and may occur only episodically [*Resplandy et al.*, 2009]. In Plate 1, these seasonal changes appear to be linked to a northward shift, the broadening and eastward extension of the thermocline ridge; a related, and more direct, linkage is with mixed-layer thickness (see section 3.3). The wintertime intensification can also be seen in Plate 5a, top left (below), which shows surface chlorophyll from SeaWiFS during 1998 averaged from 10–12°S; the bloom is present only during the austral winter, possibly because the averaging band is located too far south to pick up any of the weaker bloom during austral summer (Plate 1) or because of interannual variability.

A physical reason for the low chlorophyll values along the ridge is that, in contrast to coastal regions, upwelling velocities are weak along the ridge since the total upwelling transport is spread over such a large area; moreover, the upwelling may also be "zero," a result of the ocean adjusting to a state of Sverdrup balance in which w_{ek} no longer drives an upwelling velocity. (The adjustment to Sverdrup balance can be understood using a simple, reduced-gravity ($1\frac{1}{2}$-layer) model of the oceanic surface layer, which results in the familiar equation, $h_{1t} + c_r h_{1x} = -w_{ek}$, where $c_r = -\beta g' h_1 / f^2$. Ekman pumping is the balance between the first and third terms ($h_{1t} = -w_{ek}$), a statement that h_1 continues to thin (upwell) in response to positive Ekman pumping. Sverdrup balance is the balance between the second and third terms ($c_r h_{1x} = -w_{ek}$), for which $h_{1t} = 0$, and there is no upwelling. The balance between the first and second terms ($h_{1t} = -c_r h_{1x}$) describes a Rossby wave propagating westward at speed c_r. In response to a switched-on wind, the ocean is initially in a state of Ekman balance. Subsequently, it adjusts to a state of Sverdrup balance via the radiation of a Rossby wave. An exception to this adjustment occurs when $w_{ek} > 0$, and h_1 becomes too thin in some region, thinner than a minimum value H_m, say; in that case, $h_1 = H_m$ and $h_{1x} = 0$ there, the Ekman balance holds, and there is upwelling. Indeed, low SST values indicative of upwelling are not apparent along the ridge in climatological SST, although they do occur during intraseasonal events; see section 4.1.) A biochemical reason for the low chlorophyll is that the ridge is a region of low-iron concentration that weakens surface production [*Wiggert et al.*, 2006; *Behrenfeld et al.*, 2009]. Both the iron stress indicated in these analyses and the moderate upwelling noted above suggest that primary production in this region is localized within deep chlorophyll maxima (DCMs), which are apparent in the available in situ data [*Wiggert et al.*, this volume].

Figure 1 and Plate 1 illustrate the climatological forcing and response. There is also significant variability about this background state at both intraseasonal and interannual timescales, which also indicates systematic biophysical connections.

1.2. Present Paper

In this paper, we present an overview of biophysical interactions in the IO, discussing processes that are known, or believed, to be involved in generating many of the blooms

illustrated in Plate 1. Section 2 provides an overview of basic biophysical processes that impact biological activity, both near the ocean surface and below. Sections 3, 4, and 5 then review biophysical interactions at seasonal, intraseasonal, and interannual timescales, respectively. This division by timescale is instructive but imperfect, since phenomena at different time scales often interact significantly; for example, intraseasonal forcing has a lowest-order impact on the annual blooms in the central Arabian Sea, and so its effects are also discussed in section 3.1.2. Section 6 summarizes our results and discusses implications for future work.

Our focus is on interactions at "large" (greater than mesoscale) spatial scales. On the other hand, existing observations show significant variability at the patch scale (1–10 km) in several IO regions, with patterns suggesting the influence of fronts and eddies. These regions include the coastlines of Oman and Somalia during the SWM [e.g., *Böhm et al.*, 1999; *Lee et al.*, 2000; *Hitchcock et al.*, 2000; *Kim et al.*, 2001], the neighborhood of Sri Lanka (see Plate 2 below), the Mozambique channel [e.g., *de Ruijter et al.*, 2002; *Quartly and Srokosz*, 2004], and the Leeuwin Current [e.g., *Rennie et al.*, 2007; *Moore et al.*, 2007]. Furthermore, studies in the IO [e.g., *Waite et al.*, 2007] and other oceans point toward the important role of meso- and submesoscale processes in bloom evolution [*Garcon et al.*, 2001; *Benitez-Nelson and McGillicuddy*, 2008]. A proper review of the impact of these processes on phytoplankton bloom dynamics is not possible in the IO, due to the scarcity of observations and general lack of biophysical modeling studies that resolve mesocale and submesoscale interactions. In any case, these smaller-scale processes work on lateral and vertical gradients created by the large-scale processes discussed here. Thus, our overview provides the background upon which smaller-scale processes are active.

Our paper complements several others in this volume that discuss a variety of issues concerning biophysical interactions [e.g., *Koné et al.*, this volume; *Marra and Moore*, this volume; *Rixen et al.*, this volume; *Vinayachandran*, this volume, and *Wiggert et al.*, this volume]; in addition, *Hood et al.* [this volume] discusses a variety of outstanding research questions, many of which are related to biophysical interactions. Other papers that also provide overviews of IO biophysical interactions are *Wiggert et al.* [2006] and *Levy et al.* [2007].

2. BIOPHYSICAL INTERACTIONS

In this section, we first discuss general biophysical processes that occur within and just below the mixed layer. Then, we review the IO's shallow overturning circulations, the subsurface branches that supply water for the upwelling regions. Finally, we note the potential impacts of deeper (subthermocline) circulations on biological activity, specifically concerning the maintenance of oxygen minimum zones.

2.1. Near-Surface Processes

Figure 2 schematically illustrates the three types of blooms that can occur due to mixed-layer processes, namely, upwelling, entrainment, and detrainment blooms. Figure 2 (top) indicates changes in mixed-layer thickness h_m and the seasonal thermocline h_f (the region below the mixed layer but above the main thermocline) that typically occur during an upwelling event. Upwelling happens whenever the wind generates a divergent, surface flow that removes upper-layer water from a region. The left-hand profile shows a typical layer structure at the beginning of an upwelling event. As time passes, the mixed layer thins until h_m reaches its minimum thickness H_m (the sequence of profiles 1–4). Thereafter, water from the seasonal thermocline is entrained into the mixed layer, and h_f thins (profiles 4–6). Eventually, the seasonal thermocline layer is also eliminated, at which time upwelling from the main thermocline begins (profile 7). At this time, upwelling becomes a powerful process for generating biological activity because it brings high-nutrient, thermocline water into a thin, surface mixed layer, where the depth-averaged light intensity is high.

Figure 2 (bottom) illustrates changes due to entrainment of subsurface water into the mixed layer. Entrainment occurs whenever there is an increase in surface turbulent mixing (due either to strengthened winds or surface cooling). The left-hand profile shows a typical layer structure at the beginning of an entrainment event in which $h_m = H_m$. Fluid entrains into the mixed layer, increasing h_m until the seasonal thermocline vanishes (profiles 1–5), at which time thermocline water begins to entrain into the mixed layer (profiles 5–7). Even though entrainment can bring a considerable amount of nutrients into the upper layer, entrainment blooms are not as productive as upwelling blooms because h_m is thick and, hence, the depth-averaged light intensity is low.

Detrainment occurs whenever there is a decrease in turbulent mixing (when the wind weakens or there is surface heating), and h_m thins. This process is illustrated in Figure 2 (bottom) by reversing the order of profiles 1–5. Profile 5 shows a deep mixed layer, such as is often present after wintertime cooling; profiles 4–1 illustrate the subsequent thinning of h_m and formation of the seasonal thermocline ($h_f > 0$). Detrainment blooms tend to be highly productive because detrainment results in a thin mixed layer, thereby

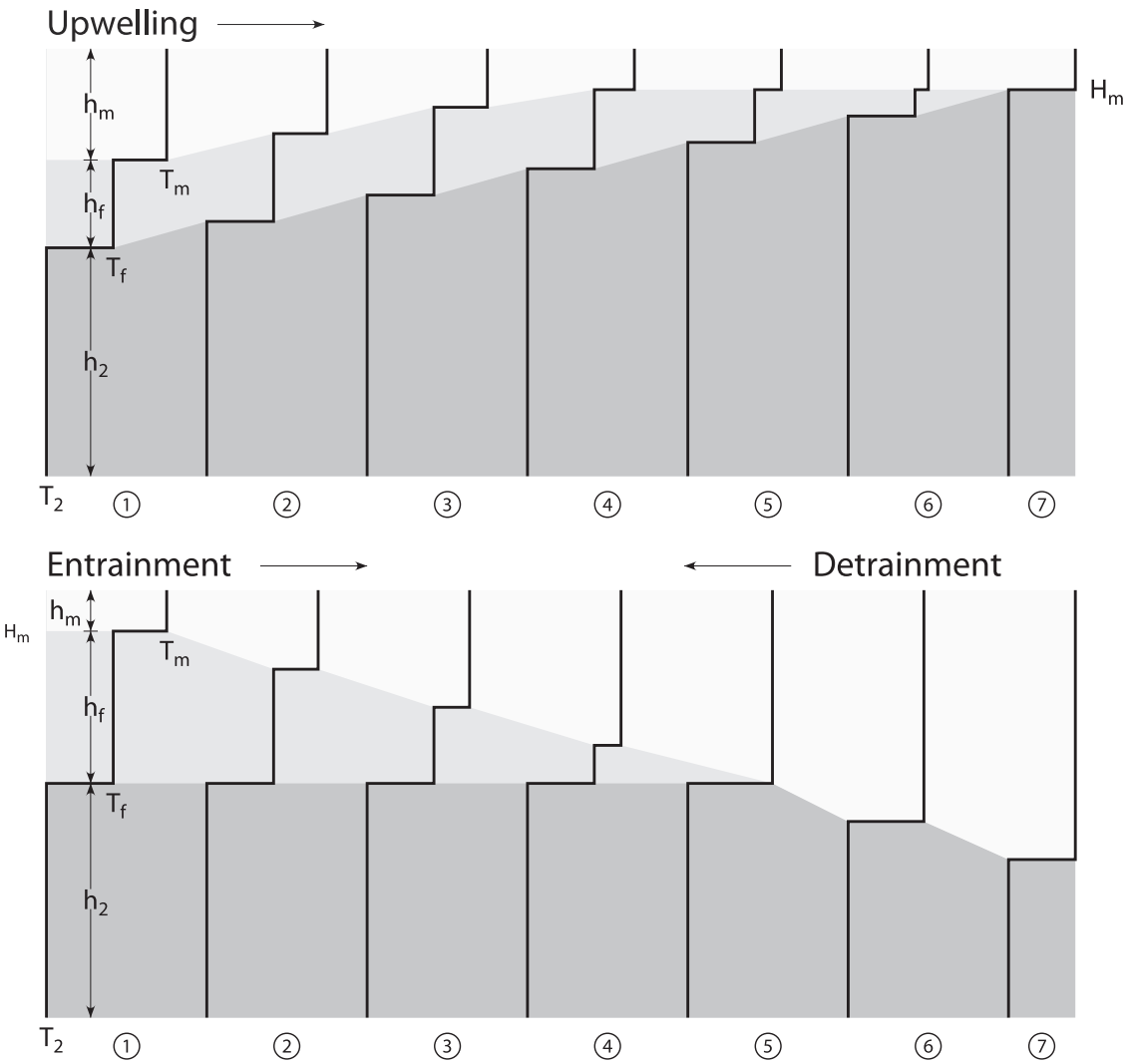

Figure 2. Schematic diagram illustrating the three types of blooms that can occur due to physics, namely, upwelling, entrainment, and detrainment blooms. The sequences of profiles indicate the changes in thicknesses of the (light shading) mixed layer h_m, (medium shading) seasonal thermocline h_f, and (heavy shading) thermocline h_2 that occur during (top) upwelling events and during entrainment and (bottom) detrainment events. For upwelling and entrainment events, the initial state is the profile at the left and time increases to the right. For detrainment events, the initial state is profile 5 in the bottom and time increases to the left. Reprinted from *McCreary et al.* [1996b], with permission from Elsevier.

favoring phytoplankton growth by increasing the depth-averaged light intensity under conditions where nutrient concentrations are typically high, the classic Sverdrup mechanism for spring blooms [*Sverdrup*, 1953]. On the other hand, they also tend to be short-lived because detrainment does not inject new nutrients into the mixed layer, and so detrainment blooms can persist only until the initial nutrient supply is depleted.

Subsurface (deep) phytoplankton maxima (DCMs) occur when the mixed layer is thin, and the thermocline (nutricline) is shallow enough to lie within the euphotic zone (similar to profiles 4–6 in Figure 2, top). Under these conditions, nutrients can become so depleted in the near-surface ocean that only minimal phytoplankton concentrations can be maintained through regenerated nutrients (see Figure 2, top); moreover, phytoplankton biomass accumulates only at

depths near the top of the nutricline. In this situation, and under the influence of some episodic atmospheric forcing, an "apparent" surface bloom can be generated simply by the entrainment of the subsurface bloom into the mixed layer. Modeling results suggest that this process occurs in the Bay of Bengal (section 3.2) [*Vinayachandran*, 2009] and in the tropical South IO during intraseasonal events (section 4).

Finally, it is well known that biological activity can be strongly impacted through advection by near-surface currents. In some cases, the impact of advection is clear, for example, with narrow streams of elevated chlorophyll extending along the edges of currents and around the perimeter of eddies (sections 3.1.1 and 3.2). As noted in the introduction, the role of advection in bloom dynamics, for example, through the advection of nutrients and other biological variables from upwelling regions (section 3.1.2), is less clear.

2.2. Shallow Overturning Cells

Shallow ($z \gtrsim -500$ m) overturning cells provide the subsurface water that surfaces in upwelling regions and, hence, are a source of nutrients for new production. In contrast to deeper overturning cells (like the Atlantic's meridional overturing circulation), the shallow cells are primarily wind-driven rather than forced by thermohaline processes. They involve the wind-driven subduction of surface water in the subtropics, subsurface flow into the tropics within the thermocline, tropical upwelling, and surface return flow to the subtropics. Although their branches (discussed next) vary considerably annually, it is their annual mean circulation that is associated with overturning, that is, diapycnal exchange (see *Schott et al.* [2004], for a review of shallow overturning cells in all oceans).

In the IO, the annual mean winds are similar in structure to, but weaker than, the July winds (Figure 1, right). They force two prominent overturning cells, the Cross-Equatorial Cell (CEC) and the Subtropical Cell (STC), which differ in the location of their upwelling branches. Figure 3 plots the meridional stream function ψ for the IO from an ocean model [*Miyama et al.*, 2003]. (Streamfunction ψ is obtained by integrating the continuity equation across the basin, thereby eliminating all contributions from the zonal currents. It follows that $V_y + W_z = 0$, where V and U are the across-basin integrations of the meridional and vertical currents, and ψ is defined by $V = -\psi_z$, $W = \psi_y$. With this definition, water flows along isolines of ψ in a direction such that lower values lie to the left.) Northward, subsurface flow crosses the equator at depths of 150–300 m to upwell in the Northern Hemisphere off Somalia, Oman, and India, forming the CEC. Another part of the subsurface flow approaches the equator, but then rises and bends southward to upwell from 5 to 10°S to form the STC. (Note the presence of a near-surface equatorial roll,

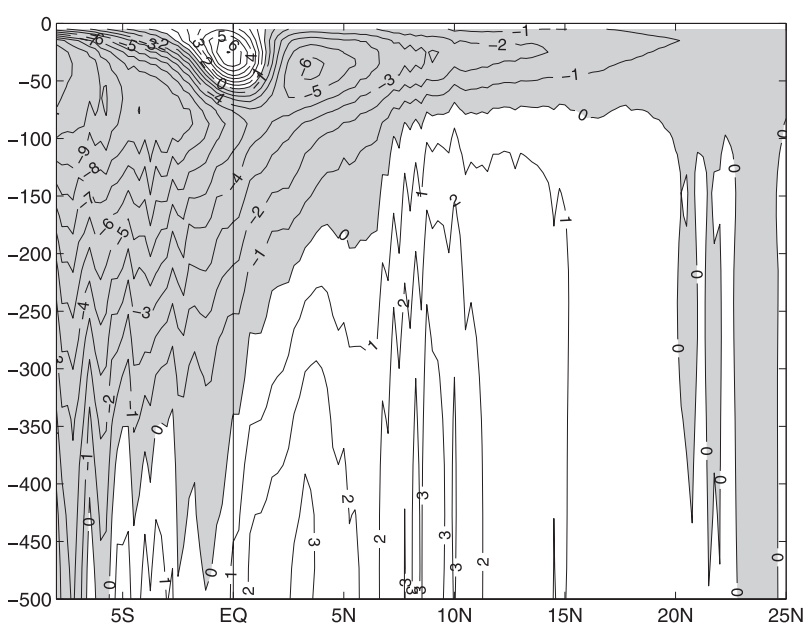

Figure 3. Annual mean meridional stream function from an ocean model. Reprinted from *Miyama et al.* [2003], with permission from Elsevier.

an interesting feature but one that is not involved in CEC or STC dynamics; see *Miyama et al.* [2003], for a recent discussion of this feature.)

The three-dimensional (3-D) flow field associated with the cells is much more complicated than suggested by the 2-D view of Figure 3 [*Schott and McCreary*, 2001; *Schott et al.*, 2004]. Their descending branch occurs in subducting regions, where *negative* Ekman pumping forces water to deepen, allowing cooler water to move under warmer water. In the IO, subduction is strongest in the southeastern basin where the westward bending of the southeast trades generates large-amplitude, negative w_{ek} (Figure 1). Available observations and models [e.g., *Schott and McCreary*, 2001; *Schott et al.*, 2004] suggest that the subducted water first flows westward in the Subtropical Gyre to the coast of Madagascar, then northward and westward to the African coast, and finally equatorward in the East African Coastal Current. Some of this water then bends offshore near 5°S to supply water for the upwelling along 5–10°S, forming the STC. The rest crosses the equator via a subsurface branch of the Somali Current to supply water for the Northern Hemisphere upwelling regions, forming the CEC. Other possible sources of water for the subsurface branch are a deep portion of the Indonesian Throughflow and inflow from the Southern Ocean [*Miyama et al.*, 2003; *Schott et al.*, 2004].

A measure of the strength of the STC is the transport of its upwelling branch. As determined from numerical simulations, the total upwelling is 5–10 Sv, a range consistent with the amplitude of the Ekman divergence there (Figure 3) [*McCreary et al.*, 1993; *Ferron and Marotzke*, 2003; *Miyama et al.*, 2003]. A measure of the strength of the CEC is the southward, cross-equatorial transport of its surface branch. As noted by *Godfrey et al.* [2001] and discussed in detail by *Miyama et al.* [2003], the zonal component of the annual mean wind stress τ^x nearly vanishes at the equator (similar to Figure 1, right), and it varies roughly proportionally with distance from the equator (that is, $\tau^x \propto y$). For this wind field, the concept of Ekman flow is valid even at the equator, since τ^x/f is well defined in the limit $y \to 0$. Moreover, it follows that $-\tau^x/f = -\tau^x_y/\beta \equiv V$ at the equator, so that the Ekman and Sverdrup transports are equal. A useful measure of CEC strength is then the integral of V along the equator, which yields a value of roughly 6 Sv [*Miyama et al.*, 2003; *Schott et al.*, 2004].

There is another region of Southern Hemispheric upwelling along the northwest Australian shelf and Arafura Sea (The shallow (50–80 m) Arafura Sea lies over the continental shelf south of New Guinea.), which generates another overturning cell. *Godfrey and Mansbridge* [2000] estimated its annual mean upwelling to be only 1.4 Sv, so that cell is weak. Finally, IOZDM episodes are marked by westward wind anomalies along the equator, which lead to upwelling in the eastern equatorial ocean and off Sumatra [*Murtugudde et al.*, 1999; *Saji et al.*, 1999; *Murtugudde et al.*, 2000; *Feng and Meyers*, 2003; *Wiggert et al.*, this volume], but their episodic contribution to the mean upwelling is small [*Schott et al.*, 2002].

2.3. Deeper Circulations

Subthermocline circulations can also affect biological processes, through their impact on biochemistry (remineralization). Perhaps the best known, subthermocline, biochemical phenomenon in the IO is the oxygen minimum zone (OMZ) in the Arabian Sea. It is one of the most intense OMZs in the present-day oceans, with near-total depletion of oxygen at depths from 200 to 1000 m [*de Sousa et al.*, 1996; *Morrison et al.*, 1999]. OMZs typically occur below regions of high productivity, where oxygen is utilized in the remineralization of sinking detritus by bacteria. A striking aspect of the Arabian Sea OMZ (ASOMZ), however, is that it is located in the eastern/central basin (65–70°W and 15–20°N), not in the western part where biological production is highest. Various hypotheses have been put forward to explain the maintenance of OMZs. On the physical side, they include the slow advection of mid-depth waters [*Sverdrup et al.*, 1942; *Olson et al.*, 1993; *Sarma*, 2002] and influx of low-oxygen deep waters from the south [*Swallow*, 1984]; on the biological side, one hypothesis is that the local ecosystem has an unusually high-oxygen demand [*Ryther and Menzel*, 1965]. The cause of the eastern shift of the ASOMZ is even less clear.

A possible explanation for the eastward shift is the presence of two prominent, subthermocline and intermediate, water masses that enter the basin from marginal seas, namely, Red Sea Water (RSW) and Persian Gulf Water (PGW). PGW spreads into the Arabian Sea just below the thermocline (250–300 m) with a core depth of $\sigma_\theta = 26.6$ kg/m^3, whereas RSW leaves the Gulf of Aden at intermediate depths (300–1000 m) with a core density of $\sigma_\theta = 27.1$–27.3 kg/m^3 [*Schott et al.*, 2002]. Both water masses are too dense to upwell within the Arabian Sea.

Neither the pathways by which PGW and RSW circulate about, and eventually leave, the Arabian Sea nor their biogeochemical signatures and impacts on the IO ecosystem are well understood. Pathways of PGW inferred from hydrographic (T/S) data suggest that PGW flows both southward along the Omani coast as well as around the perimeter of the basin [*Shenoi et al.*, 1993; *Prasad et al.*, 2001], but it is difficult to trace PGW water into the southern Arabian Sea [*Schott and McCreary*, 2001]. Pathways of RSW based on hydrographic data suggest that RSW is present all across the

basin [*Shenoi et al.*, 1993]. Both of these newly ventilated, water masses have high-oxygen content, and they may act to weaken the ASOMZ in the western basin.

3. CLIMATOLOGICAL PROCESSES

3.1. Arabian Sea

The Arabian Sea varies from calm, stratified, oligotrophic conditions during the intermonsoon periods (March–April and October–November) to strongly forced, eutrophic conditions during the SWM and NEM [*Smith et al.*, 1998]. Furthermore, the two monsoons themselves generate distinctly different biological responses. Because of its extreme variations, Arabian Sea physics and biology have captured the interest of researchers for decades, and a number of international programs have been undertaken in the region. One of the most influential programs was the U.S. Joint Global Ocean Flux Study (U.S. JGOFS) Arabian Sea Process Study (ASPS), which studied Arabian Sea biology, chemistry, and upper ocean physics during 1994–1996 [*Smith*, 2001]. In addition to enhancing the region's database, the ASPS program spurred a number of modeling studies using a variety of model types [*McCreary et al.*, 1996b, 2001; *Ryabchenko et al.*, 1998; *Murtugudde et al.*, 1999; *Wiggert et al.*, 2002, 2006; *Kawamiya and Oschlies*, 2003; *Hood et al.*, 2002]. Here, we summarize results concerning biophysical interactions from these studies, with most of the discussion focused on the blooms that occur in the central basin [see also the recent review of Arabian Sea bloom dynamics by *Wiggert et al.*, [2005]).

3.1.1. Somalia and Oman. During the SWM, the intense southwesterly winds in the western Arabian Sea (Findlater Jet; Figure 1, right) drive upwelling along the Somali and Omani coasts (In contrast, during the NEM downwelling-favorable alongshore winds inhibit coastal production.). The alongshore winds are so strong off Somalia that the upwelling circulation is "distorted" by advection into a series of upwelling wedges located between large-scale (~500 km) gyres, the most prominent of which is the Great Whirl [see, for example, *Schott and McCreary*, 2001]. Blooms, generated in the upwelling wedges, are subsequently advected well offshore around the perimeter of the gyres.

The alongshore winds are weaker off Oman, and the coastal response is more typical, with upwelling occurring everywhere along the coast and chlorophyll-rich filaments (squirts and jets) extending several hundred kilometers off the coast [*Gundersen et al.*, 1998; *Manghnani et al.*, 1998; *Lee et al.*, 2000]. Only now are models being developed with enough spatial resolution to represent the filaments adequately. Nevertheless, the potential importance of filaments in advecting biological variables offshore has been demonstrated in several modeling studies [*Young and Kindle*, 1994; *Keen et al.*, 1997; *Kindle et al.*, 2002].

3.1.2. Central Arabian Sea. During both monsoons, the mixed layer in the central Arabian Sea thickens to 50–150 m, thereby increasing nutrient concentrations but also decreasing the depth-averaged light intensity experienced by phytoplankton. At these times, primary production can be either light or nutrient limited, and so is particularly sensitive to fluctuations in mixed-layer thickness [*Marra et al.*, 1998; *Murtugudde et al.*, 2007].

McCreary et al. [2001] explored the biophysics of the offshore blooms, using a $4\frac{1}{2}$-layer physical model coupled to a nutrient, photoplankton, zooplankton, and detritus (NPZD) biological model. Figure 4 plots time series of layer thicknesses and upper layer biological variables at (61.5°E, 15.5°N) in the central Arabian Sea, the location of the WHOI mooring during the ASPS experiment. The figure contrasts two solutions that differ only in the nature of the forcing: Solution 1 driven by climatological forcing fields (Figures 4a and 4b) and Solution 2 driven by diurnal heating and daily winds (Figures 4c and 4d).

In Solution 1, the upper layer thickness h_1 increases at the beginning of the SWM due to entrainment caused primarily by wind stirring (thick curve in Figure 4b). It continues to thicken until the end of August, when detrainment due to weaker winds and warming at the end of the SWM rapidly thins h_1. During the NEM, there is another cycle of thicker h_1, in this case, due to entrainment is forced primarily by surface cooling. The cycle ends in the spring when h_1 thins due to surface heating.

The entrainment mixes high, subsurface (thermocline) nutrient concentrations into the upper layer during both monsoons, and as a result, N_1 increases continuously throughout the winter and summer (thin curve, top). In response to the initial entrainment, P_1 develops blooms that peak in early November and June (thick curve, top). Despite the high-nutrient levels, these "entrainment" blooms are short-lived because the entrainment continues to increase h_1, thereby reducing the depth-averaged light intensity sensed by the phytoplankton. Consequently, strong blooms do not occur until h_1 detrains at the end of the monsoons. These spring and fall "detrainment" blooms are intense because of the buildup of high-N_1 levels during summer, but short-lived because of the rapid depletion of N_1 and grazing by zooplankton Z_1 (dashed curve). Similar processes associated with the typical seasonal bloom dynamics of the Arabian Sea have been described in several recent ecosystem model studies; these have recently been reviewed and contrasted by *Wiggert et al.* [2005].

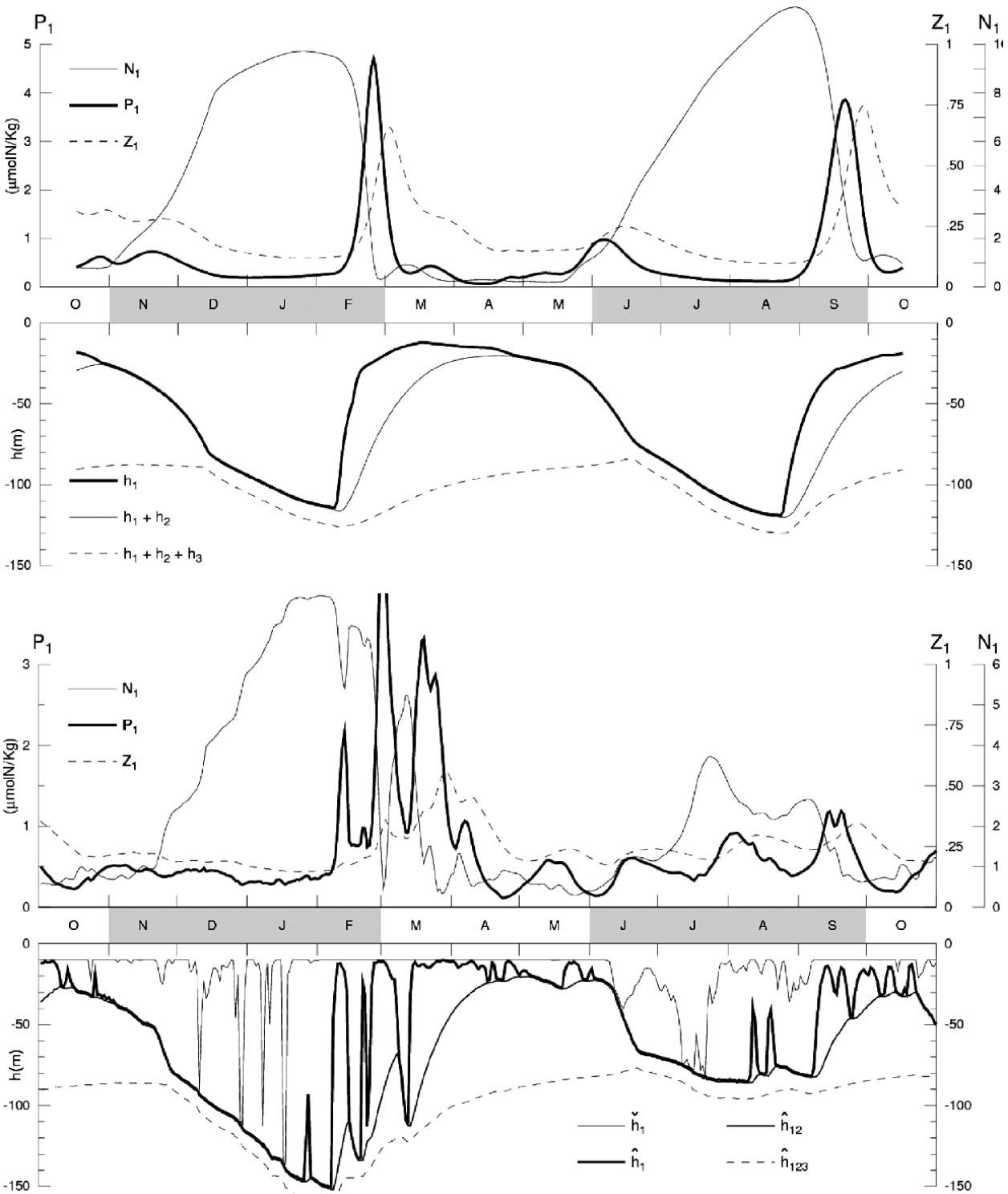

Figure 4. Time plots of layer thicknesses and upper layer biological variables in the central Arabian Sea (61.5°E, 15.5°N) from solutions to the *McCreary et al.* [2001] model forced by (a, b) climatological fields and (c, d) when the forcing also includes diurnal and intraseasonal variability. In the bottom, there are two curves for h_1, indicating its maximum ($\hat{h}_1$; thick line) and minimum ($\check{h}_1$; thin line) values on any given day. Curves $\hat{h}_{12}$ and $\hat{h}_{123}$ are the maximum daily values of $h_1 + h_2$ and $h_1 + h_2 + h_3$, respectively. Curves for the biological variables are their daily averaged values. Shading indicates typical times of the monsoon periods. From *McCreary et al*. [2001].

In Solution 2, the overall annual structure of $\hat{h}_1$ (the daily maximum of h_1) is similar to that of h_1 in Solution 1. One apparent difference is the existence of pulses of thinner $\hat{h}_1$ during the monsoons, particularly the NEM, associated with break periods in the wind forcing (thick curve, bottom). There are times when $\hat{h}_1$ thickens more rapidly associated with strong wind events; they are also accompanied by a thickening of $\hat{h}_1$ (the daily minimum of h_1), except during the intermonsoons. The spring bloom is now divided into three prominent peaks (P_1, lower middle), each of which is a "detrainment" bloom corresponding to periods when $\hat{h}_1$ thins for a week or more (thick curve, lower middle). As a consequence, the overall spring bloom lasts much longer than in Solution 1, extending from February throughout March. Note that the individual bloom events rapidly deplete the nutrient supply N_1, but that N_1 is quickly replenished by subsequent entrainment (thin curve, lower middle). The fall bloom is also broadened in time, but by several "entrainment" blooms corresponding to periods when $\hat{h}_1$ thickens more rapidly. In addition to the initial entrainment bloom in June, there is a second one in July/August, which results from intensified winds in mid-July that deepen $\hat{h}_1$ by about 10 m. Remarkably, there is observational support for intraseasonal detrainment and entrainment blooms in satellite ocean-color data (section 4.1).

There has been considerable discussion about the impact of forcing by the strong positive Ekman pumping w_{ek} northwest of the axis of the Findlater Jet during the SWM (Figure 1, right) on thermocline depth and bloom dynamics. The positive w_{ek} has been noted as a possible source of upwelling just offshore from Oman [*Smith and Bottero*, 1977; *Brock et al.*, 1991; *Bauer et al.*, 1991]. Based on their model solutions, however, *McCreary et al.* [1996b] concluded that upwelling driven by w_{ek} was not significant off Oman (in comparison to the coastal upwelling there), likely because the system had adjusted toward a state of Sverdrup balance in which Ekman pumping no longer drives upwelling (see parenthetical discussion in section 1.1, paragraph 8).

Similarly, there has been discussion about the relative importance of negative Ekman pumping in deepening the offshore thermocline. Whether surface convergence (negative w_{ek}) or entrainment is the process that thickens h_1 is biologically important, since the former does not bring additional nutrients into the upper layer; furthermore, negative w_{ek} may deepen the thermocline so much that it is difficult for entrainment to mix nutrients from the nutricline into the mixed layer (profiles 1–4 in Figure 2, bottom) [*Murtugudde et al.*, 2007]. During the SWM, there is negative w_{ek} southeast of the axis of the Findlater Jet. *McCreary et al.* [1996b] noted that h_1 in their solution (very similar to h_1 in Plate 1, bottom right) attained relative maxima near the zero line of w_{ek}, indicating the importance (dominance) of entrainment. *Murtugudde et al.* [2007] concluded that both processes are active.

Another issue is the relative importance of local entrainment vs. advection from coastal upwelling regions as nutrient sources for the central Arabian Sea during the SWM. To explore this issue, *McCreary et al.* [1996b] obtained a test solution without advection in the equation for mixed-layer nutrients. The resulting nutrient buildup in the central Arabian Sea was considerably less but not zero, pointing toward significant contributions from both sources. *Murtugudde et al.* [1999] and *Wiggert et al.* [2002] also invoke offshore advection of nutrients from the coast in order to explain the high levels of primary production in the central Arabian Sea. A more complete assessment and inclusive discussion of the various mechanisms proposed in the literature is by *Wiggert and Murtugudde* [2007].

3.1.3. West coast of India. Biological activity is very different between the northern and southern parts of the Indian west coast [*Levy et al.*, 2007]. Along the southern coast, blooms occur only during the SWM. At that time, the local winds do have an upwelling-favorable (northwesterly) component there (Figure 1, right), but they are too weak in themselves to drive the upwelling [*McCreary et al.*, 1993; *Shankar and Shetye*, 1997; *Shankar et al.*, 2002]. The major forcing for the upwelling, as well as for the southward-flowing West India Coastal Current (WICC), comes from the much stronger, upwelling-favorable winds in the Bay of Bengal, which lift the thermocline along the west coast via the propagation of coastal Kelvin waves (section 1) [*McCreary et al.*, 1993; *Shankar and Shetye*, 1997). A related bloom in the Lakshadweep Sea, which lags the coastal bloom by about 2 months, has also been observed [*Lierheimer and Banse*, 2002; *Levy et al.*, 2007]; it appears to be driven by upwelling caused by the offshore radiation of Rossby waves from the Indian coast. (The Lakshadweep Sea lies between the southwest coast of India and the Chagos-Laccadive ridge (~72°E), the same ridge that contains the Maldive islands farther south. The southern limit of the Lakshadweep Sea coincides with the southern tip of India at 8°N and its northern limit is at 13°N.)

Along the northern coast, there are blooms during both monsoons. During the NEM, they are driven by entrainment caused by winter cooling and the associated convective mixing (section 3.1.2) [*Banse*, 1984; *Shetye et al.*, 1992; *Madhupratap et al.*, 1996). During the SWM, they are also driven by entrainment, in this case due to strong winds that promote mechanical mixing (Figure 1, right); note that the SWM winds blow almost directly onshore there, so that upwelling (which is driven by alongshore winds) is not likely to be significant. They are also likely to be partly remotely

forced by Kelvin waves propagating from the south, which act to shallow the northern coastal thermocline (*Shankar et al.*, 2002).

3.2. Bay of Bengal and Sri Lanka

Blooms and productivity in the Bay of Bengal and near Sri Lanka, although weaker than those in the Arabian Sea, are noteworthy in a number of aspects. Here, we comment on two examples. See *Vinayachandran* [this volume] for a detailed overview.

Biological productivity in the Bay is weaker because the Bay lacks a strong upwelling system. As noted in the introduction, one reason for the weaker upwelling is that the winds along the east coast of India are weaker than along Somalia and Oman, and another is the remotely forced deepening of the thermocline around the perimeter of the Bay (Plate 1, bottom right). A third cause is the large freshwater flux into the Bay, which stratifies the near-surface ocean and, hence, acts to inhibit upwelling of nutrient-rich, thermocline water.

Nevertheless, there are blooms of lesser intensity in the Bay. A significant example occurs in the southwestern Bay during the NEM [*Vinayachandran and Mathew*, 2003]. *Vinayachandran et al.* [2005] used a coupled, biophysical model to investigate its dynamics. In early November, the thermocline and nutricline are shallow, under the influence of positive w_{ek} earlier in the year, and the mixed layer is thin [*McCreary et al.*, 1996b; *Vinayachandran and Yamagata*, 1998]. Under these conditions, a subsurface bloom develops initially. Subsequently, this chlorophyll-rich, subsurface water can be entrained into the mixed layer, especially during strong upwelling-favorable wind events in the open ocean, thereby contributing significantly to surface blooms. Indeed, in the *Vinayachandran et al.* [2005] model, a surface bloom does not develop at all when the supply of phytoplankton from the subsurface maximum is not permitted into the mixed layer (see the discussion of their Figure 7). Other blooms in the Bay are related to the passage of cold-core eddies and cyclones, the former raising the thermocline and nutricline (section 4.2) [*Prasanna Kumar et al.*, 2004] and the latter thickening the mixed layer by entrainment.

As noted in the introduction, the bloom near Sri Lanka during the SWM (Plate 1, right) is partly caused by upwelling forced by Ekman suction, but other processes are important as well [*Vinayachandran et al.*, 2004]. Plate 2 illustrates the complexity of the bloom, showing its structure on 29 July 1999. There are upwelling blooms along the southwest coast of India (section 3.1.3) and the southern coast of Sri Lanka. Chlorophyll-rich water from both regions is transported by the eastward-flowing Southwest Monsoon Current (SMC) around Sri Lanka and into the Bay of Bengal [*Vinayachandran et al.*, 1999; *Shankar et al.*, 2002; *Levy et al.*, 2007]. East of Sri Lanka, open-ocean Ekman pumping within the Sri Lanka dome (a region just east of Sri Lanka where the thermocline is particularly shallow) also caused a bloom.

3.3. Southern Hemisphere

In the MKM model, the thermocline rises to its minimum thickness of 35 m over much of the thermocline ridge (Plate 1, bottom), allowing upwelling to occur, albeit with weak upward velocities. In other ocean models and observations, the ridge approaches but does not reach the surface, an indication that the ocean may adjust to a state of Sverdrup balance without upwelling (see the parenthetical discussion in section 1.1, paragraph 8). These conditions (shallow thermocline, weak or no upwelling) favor the development of a DCM. Indeed, model results suggest that DCMs prevail throughout the region. For example, *Kawamiya and Oschlies* [2001] and *Wiggert et al.* [2006] report prominent DCMs in their solutions in the southern tropical IO, which in the latter study exists throughout the year except during August–October. Unfortunately, in situ observations are too limited to confirm these modeling results. During an oceanographic cruise of the Cirene program (January–February 2007), however, a DCM was observed to be present along the ridge from 55 to 70°E with an average depth of 80 m and concentration of 0.3 mg/m^3; in contrast, average concentrations at the surface and in the mixed layer were only 0.05 mg/m^3 [*Vialard et al.*, 2009; *Wiggert et al.*, this volume]. It should be noted, however, that the 5–10°S ridge region had a deeper than usual thermocline during Cirene as a result of the 2006 IOZDM event and that the subsurface *P* maxima was most likely deeper and weaker than usual as a result [*Vialard et al.*, 2009].

Given the presence of the DCM, two processes might explain the existence of surface blooms from 5 to 20°S during austral winter: entrainment of either nutrients or phytoplankton from the DCM into the mixed layer. Based on their modeling study, *Resplandy et al.* [2009] suggest that the former process dominates. Interestingly, there is a wintertime decrease in DCM strength in their solution; it does not result from entrainment loss to the surface layer, but rather from wintertime reduction in photosynthetically active radiation (PAR) and from subsurface shading by the surface bloom. Both *Kawamiya and Oschlies* [2001] and *Resplandy et al.* [2009] concluded that surface blooms in the region are weaker during the austral summer (Plate 1, top) because the mixed layer is thinner in response to weaker winds, and the thermocline is deeper; as a result, it is rare for typical mixing events to extend to the depth of the nutricline.

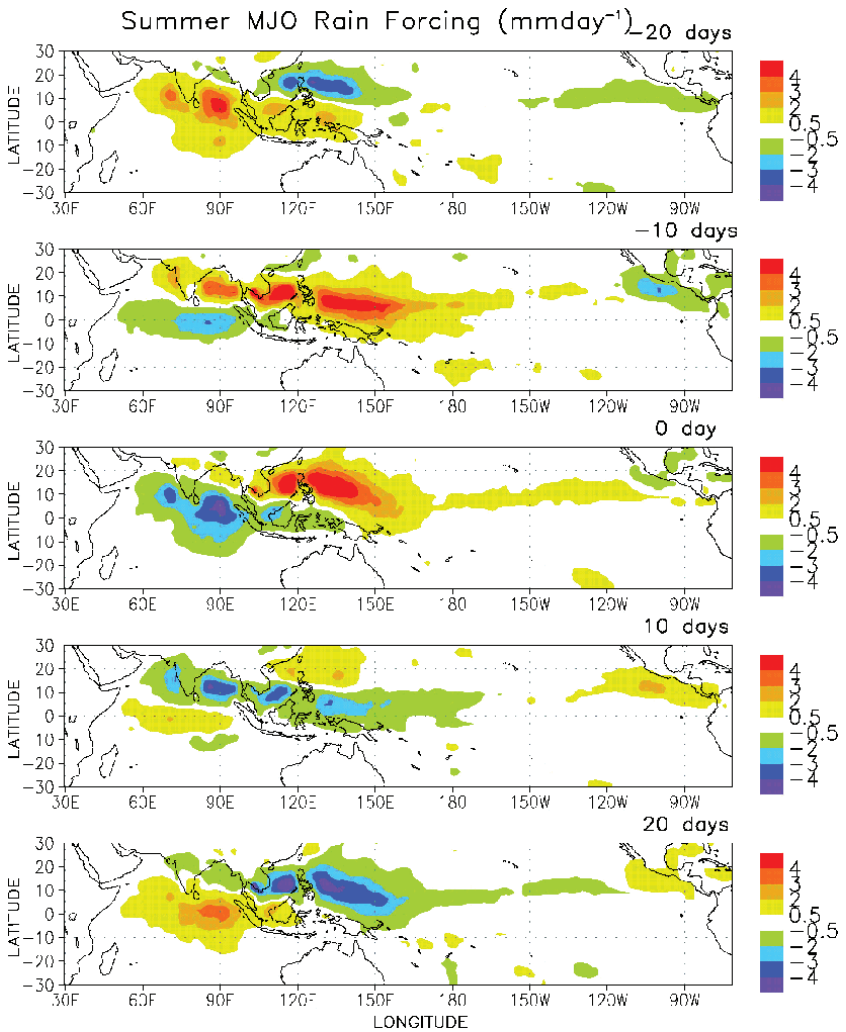

Plate 3a. Maps of anomalous rainfall for 13 summer MJOs from 1998 to 2004, illustrating the time development of typical MJO events. The patterns originate in the western IO, propagate eastward and northward across the basin, and weaken in the Pacific Ocean. Their arrival time in the eastern IO is defined to be $t = 0$. From *Waliser et al.* [2005].

4. INTRASEASONAL VARIABILITY

Ecosystem variability at intraseasonal (and higher) frequencies remains largely unexplored. Several recent studies, though, have shown that biological activity is linked to physical variability even at these shorter timescales. The physical variability is both externally forced by intraseasonal winds, notably by Madden-Julian Oscillations (MJOs) [*Madden and Julian*, 1971, 1972, 1994, 2005] and internally generated by the passage of oceanic Rossby waves and eddies [*Kawamiya and Oschlies*, 2001; *Jochum and Murtugudde*, 2005; *Zhou et al.*, 2008]; see *Kessler* [2005] for a recent review of oceanic intraseasonal variability.

4.1. Response to MJOs

The MJOs, arguably the most prominent intraseasonal oscillations in the tropical atmosphere, are eastward-propagating, convective disturbances with periods of 40–60 days. Their impacts on rainfall, oceanic surface fluxes, and SST are well documented [e.g., *Waliser et al.*, 2005]. Plate 3a presents maps of anomalous precipitation composited for 13 boreal summer MJOs from 1998–2004 and clearly illustrates their large-scale nature. The panels correspond to phases of the composite MJO separated by 10 days, with $t = 0$ being the time that convection arrives in the eastern ocean. During summer, MJOs propagate northward as well as eastward,